Cell Reports

Article

The Methyltransferase DOT1L Controls Activation and Lineage Integrity in CD4$^+$ T Cells during Infection and Inflammation

Graphical Abstract

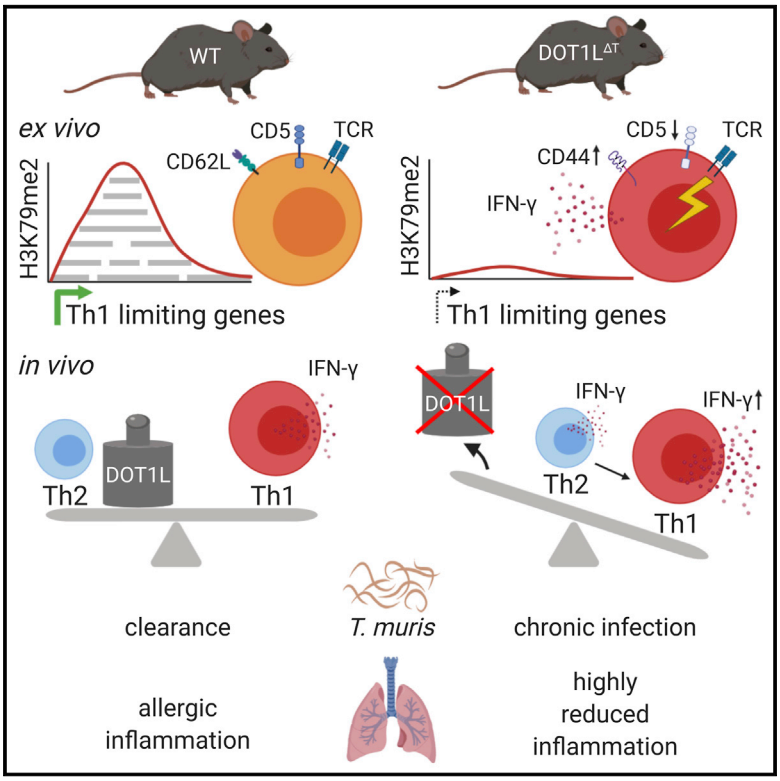

Highlights

- DOT1L restricts activation of peripheral CD4$^+$ T cells
- DOT1L regulates expression of the Th1 cell gene program
- DOT1L limits lineage-promiscuous IFN-γ expression
- DOT1L$^{\Delta T}$ mice show impaired worm clearance and reduced lung inflammation

Authors

Sebastian Scheer, Jessica Runting, Michael Bramhall, ..., Grace Rodrigues, Judy Ng, Colby Zaph

Correspondence

sebastian.scheer@monash.edu (S.S.), colby.zaph@monash.edu (C.Z.)

In Brief

Scheer et al. show that the lysine methyltransferase DOT1L has a central role in regulating T helper cell activation and lineage integrity by controlling T cell receptor reactivity and expression of the Th1 gene program.

Scheer et al., 2020, Cell Reports *33*, 108505
December 15, 2020
https://doi.org/10.1016/j.celrep.2020.108505

CellPress

Cell Reports

CellPress
OPEN ACCESS

Article

The Methyltransferase DOT1L Controls Activation and Lineage Integrity in CD4$^+$ T Cells during Infection and Inflammation

Sebastian Scheer,[1,3,*] Jessica Runting,[1,3] Michael Bramhall,[1,3] Brendan Russ,[1,2] Aidil Zaini,[1,3] Jessie Ellemor,[1,3] Grace Rodrigues,[1,3] Judy Ng,[1,3] and Colby Zaph[1,3,4,*]

[1]Infection and Immunity Program, Monash Biomedicine Discovery Institute, Clayton, VIC 3800, Australia
[2]Department of Microbiology, Monash University, Clayton VIC 3800, Australia
[3]Department of Biochemistry and Molecular Biology, Monash University, Clayton VIC 3800, Australia
[4]Lead Contact
*Correspondence: sebastian.scheer@monash.edu (S.S.), colby.zaph@monash.edu (C.Z.)
https://doi.org/10.1016/j.celrep.2020.108505

SUMMARY

CD4$^+$ T helper (Th) cell differentiation is controlled by lineage-specific expression of transcription factors and effector proteins, as well as silencing of lineage-promiscuous genes. Lysine methyltransferases (KMTs) comprise a major class of epigenetic enzymes that are emerging as important regulators of Th cell biology. Here, we show that the KMT DOT1L regulates Th cell function and lineage integrity. DOT1L-dependent dimethylation of lysine 79 of histone H3 (H3K79me2) is associated with lineage-specific gene expression. However, DOT1L-deficient Th cells overproduce IFN-γ under lineage-specific and lineage-promiscuous conditions. Consistent with the increased IFN-γ response, mice with a T-cell-specific deletion of DOT1L are susceptible to infection with the helminth parasite *Trichuris muris* and are resistant to the development of allergic lung inflammation. These results identify a central role for DOT1L in Th2 cell lineage commitment and stability and suggest that inhibition of DOT1L may provide a therapeutic strategy to limit type 2 immune responses.

INTRODUCTION

Upon encounter of foreign antigens in the periphery, CD4$^+$ T helper (Th) cells can differentiate into several cell lineages that have distinct physiological properties and functions (Zhu et al., 2010). For example, Th1 cells are induced after viral or intracellular bacterial infection, produce the cytokine interferon-γ (IFN-γ), and activate macrophages to kill infectious organisms. In contrast, Th2 cells express interleukin (IL)-4, IL-5, and IL-13 after helminth infection and are required for immunity to this class of pathogens. These cells show a distinct and mutually exclusive cell fate because the induction of the Th1 cell lineage program by the cytokine IL-12 and the transcription factor (TF) TBET leads to the production of IFN-γ and represses genes that characterize differentiated Th2 cells, such as IL-4 and IL-13 and the TF GATA3. Maintenance of lineage integrity is critical for optimal responses to a wide variety of pathogens. In addition, an imbalanced Th1/Th2 immune response may be responsible for the onset or maintenance of T-cell-mediated inflammatory disorders.

Epigenetic modifiers, such as histone lysine methyltransferases (KMTs) have emerged as critical regulators of Th cell differentiation and function because their activity results in a defined state of chromatin, which enables the regulation of gene expression and, in turn, regulates cellular development and differentiation (He et al., 2013). We and others have previously shown that modulation of KMT activity has a profound effect on Th cell differentiation, lineage stability, and function. For example, EZH2-dependent trimethylation of histone H3 at lysine 27 (H3K27me3) and SUV39H1/2-dependent H3K9me3 are important for lineage integrity of Th1 and Th2 cells (Allan et al., 2012; Tumes et al., 2013), whereas G9a-mediated H3K9me2 has been shown to control regulatory T cell (T_{reg}) and Th17 cell differentiation (Antignano et al., 2014; Lehnertz et al., 2010). Importantly, KMTs are viable drug targets in a wide range of diseases (Schapira and Arrowsmith, 2016). Thus, a better understanding of the epigenetic mechanisms controlling Th cell differentiation and lineage stability could offer new strategies to modulate dysregulated Th cell function in disease.

Recently, in a screen using chemical probes targeting KMTs, H3K79 methyltransferase Disruptor of telomeric silencing 1-like (DOT1L) was shown to limit Th1 cell differentiation in both murine and human Th cells *in vitro* (Scheer et al., 2019). DOT1L is the sole KMT for H3K79, performing mono-, di-, and trimethylation *in vivo* (Frederiks et al., 2008; Min et al., 2003) because its knockout leads to a complete loss of H3K79 methylation (Jones et al., 2008). DOT1L-dependent H3K79 methylation has been suggested to directly promote transcriptional activation (Guenther et al., 2007; Steger et al., 2008). However, H3K79me2 has also been correlated to silenced genes (Zhang et al., 2006) and was further associated with both gene activation and repression in the same cell for separate genes (Chen et al.,

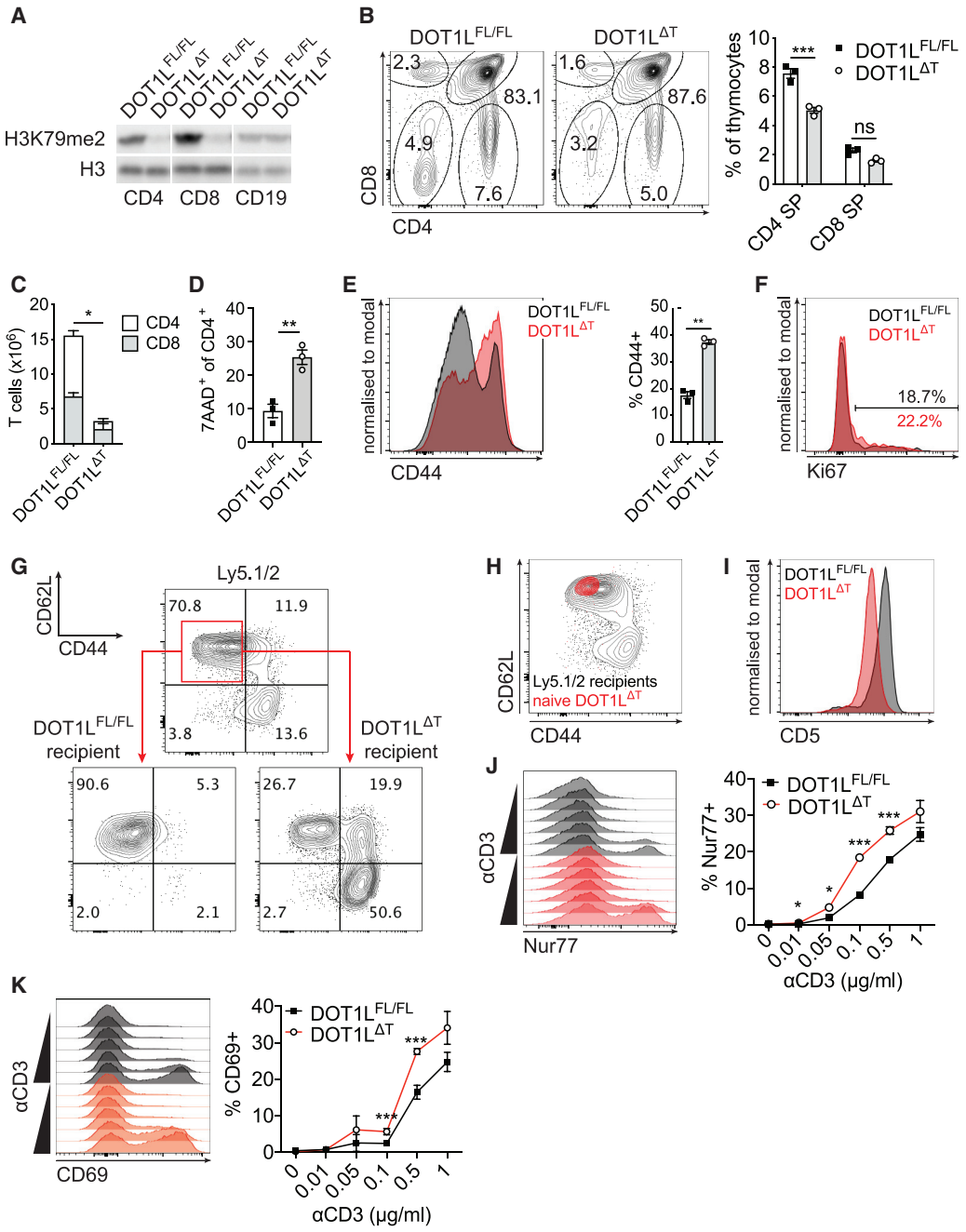

Figure 1. DOT1L Restricts Activation of Peripheral CD4⁺ T Cells

(A) Western blot of histone extracts from sorted TCRβ⁺ CD4⁺ (CD4) and TCRβ⁺ CD8⁺ (CD8) T cells and CD19⁺ B cells (CD19) from control (DOT1L$^{FL/FL}$) or T-cell-conditional knockout mice for DOT1L (DOT1L$^{\Delta T}$) for H3K79me2 and pan-H3 (control).

(B) FACS-analysis of the thymi of DOT1L$^{FL/FL}$ and DOT1L$^{\Delta T}$ mice (left) and quantification of CD4 single-positive (SP) and CD8SP thymocytes (right).

(C) Absolute numbers of splenic CD4⁺ and CD8⁺ T cells from DOT1L$^{FL/FL}$ and DOT1L$^{\Delta T}$ mice.

(D) Splenic 7AAD⁺ CD4⁺ T cells in DOT1L$^{FL/FL}$ and DOT1L$^{\Delta T}$ mice.

(E) Histogram for expression of CD44 (activated cells) of splenic CD4⁺ T cells (left) and quantification (right).

(F) Histogram for Ki67 expression of splenic CD4⁺ CD44⁺ CD62L^{low} T cells.

(G) Analysis of the spleens 7 days after adoptive transfer of FACS congenic (Ly5.1/2⁺; donor), naive (CD44⁻ CD62L^{high}) CD4⁺ T cells into either DOT1L$^{FL/FL}$- or DOT1L$^{\Delta T}$-recipient mice for their expression of CD62L and CD44. Splenic CD4⁺ T cells of non-recipient DOT1L$^{FL/FL}$ or DOT1L$^{\Delta T}$ control mice are indicated. Red box indicates sorted, naive cells that were transferred into either DOT1L$^{FL/FL}$- or DOT1L$^{\Delta T}$-recipient mice (see arrows).

(H) Analysis of the spleen of a congenic Ly5.1/2⁺-recipient mouse 7 days after adoptive transfer of FACS, naive (CD44⁻ CD62L^{high}) DOT1L-deficient splenic CD4⁺ T cells (DOT1L$^{\Delta T}$ donor mice) for expression of CD62L and CD44.

(legend continued on next page)

2020). These reports highlight the lack of clarity of H3K79 methylation in mammalian gene transcription, and the role of H3K79 methylation in Th cells has not been described in detail. In addition, the *in vivo* role of DOT1L in T cells is unknown, and a better understanding of the function of DOT1L may lead to the development of new therapeutics against inflammatory disorders mediated by dysregulated T cell responses.

Here, we identify a key role for DOT1L in limiting T cell activation and the Th1 cell differentiation program in effector Th cells. DOT1L-dependent H3K79me2 is associated with lineage-specific gene expression in Th cells. However, loss of DOT1L results in increased production of Th1-cell-associated genes and IFN-γ production under both lineage-specific and -promiscuous conditions. Further, the absence of DOT1L in Th cells leads to an increased Th1 and an impaired Th2 cell response during infection with the helminth parasite *Trichuris muris* or during allergic airway inflammation, identifying DOT1L as a potential therapeutic target to treat diseases associated with dysregulated Th2 cell responses at mucosal sites.

RESULTS

DOT1L Restricts Activation of CD4$^+$ T Cells in the Periphery

To begin to understand the precise role of DOT1L and H3K79 methylation in Th cell differentiation, we generated a T-cell-specific DOT1L-deficient mouse strain (DOT1L$^{\Delta T}$ mice) by crossing *Dot1l*$^{fl/fl}$ mice with *Cd4*-Cre transgenic mice, resulting in a specific reduction in DOT1L-dependent H3K79me2 levels within peripheral T cells (Figure 1A). Analysis of thymic T cells shows a slight, yet not significant, reduction of CD8 single-positive (SP) cells in DOT1L$^{\Delta T}$ mice compared with DOT1L$^{FL/FL}$ mice, whereas the frequency of CD4SP thymocytes is significantly decreased in DOT1L$^{\Delta T}$ mice (Figure 1B). In addition, CD4SP, but not CD8SP, cells showed increased cell death (7AAD$^+$; Figure S1A), suggesting that DOT1L is specifically important for the survival of CD4SP thymocytes.

To investigate the downstream effect of decreased frequency of CD4SP cells in the thymus of DOT1L$^{\Delta T}$ mice on the pool of peripheral T cells, we analyzed the spleens of DOT1L$^{\Delta T}$ mice and found that the cell numbers and frequencies of CD4$^+$ T cells were significantly reduced in the absence of DOT1L (Figure 1C). In addition to increased cell death in thymocytes in the absence of DOT1L, splenic CD4$^+$ T cells also showed increased cell death (7AAD$^+$), further supporting the importance of DOT1L in T cell survival (Figure 1D). Peripheral CD4$^+$ T cells presented with an increased, activated CD44^{hi} phenotype (Figure 1E), showing that the presence of DOT1L may act to limit CD4$^+$ T cell activation. T cell lymphopenia can lead to the activation and proliferation of remaining cells (Voehringer et al., 2008). Because increased CD44 expression of splenic CD4$^+$ T cells in the absence of DOT1L was not due to increased proliferation (Figure 1F, gated on CD44$^+$ CD62L^{low}), we next tested whether the lymphopenic environment of DOT1L$^{\Delta T}$ mice would lead to the activation of naive congenic CD4$^+$ T cells (CD44$^-$ CD62L^{high}, Ly5.1/2$^+$). Consistent with the activated phenotype of splenic CD4$^+$ T cells in DOT1L$^{\Delta T}$ mice, we observed a highly activated phenotype (CD44$^+$ CD62L^{low}) of injected naive (CD44$^-$ CD62L^{high}) cells after 1 week in recipient DOT1L$^{\Delta T}$ mice (Figure 1G). In contrast, we found that adoptive transfer of naive (CD44$^-$ CD62L^{high}) DOT1L-deficient CD4$^+$ T cells into congenic wild-type (WT) recipients does not result in their activation (Figure 1H). Taken together, these results suggest that the activated phenotype of CD4$^+$ T cells in DOT1L$^{\Delta}$ mice is not due to the absence of DOT1L in peripheral T cells but rather is caused by the lymphopenic conditions.

To investigate the role of T cell receptor (TCR) signaling for the activated phenotype of CD4$^+$ T cells in DOT1L$^{\Delta T}$ mice, we analyzed the TCR signaling capacity of peripheral CD4$^+$ T cells. We found that expression of the negative regulator of TCR signaling (Voisinne et al., 2018), CD5, was highly reduced in DOT1L-deficient CD4$^+$ T cells (Figure 1I). Because expression of CD5 in SP CD4$^+$ thymocytes from DOT1L$^{\Delta T}$ mice is similar to that of WT controls (Figure S1B) and T cells are more responsive in the absence of CD5 (Peña-Rossi et al., 1999), an increased signaling capacity through the TCR in peripheral CD4$^+$ T cells in the absence of DOT1L is suggested. To analyze the signal strength of the TCRs of peripheral CD4$^+$ T cells, we analyzed isolated splenic CD4$^+$ T cells after culturing with various levels of TCR stimulation (increasing the amounts of plate-bound αCD3) in the presence of IL-2 for Nur77 and the early activation marker CD69 (Ashouri and Weiss, 2017). After 4 h of stimulation, Nur77 and CD69 expression were higher in CD4$^+$ T cells from DOT1L$^{\Delta T}$ mice compared with that of WT controls (Figures 1J and 1K). To determine whether the lymphopenic conditions in the DOT1L$^{\Delta T}$ mice contribute to the increased TCR sensitivity of DOT1L-deficient CD4$^+$ T cells, we sorted naive (CD44$^-$ CD62L^{high}) CD4$^+$ T cells from DOT1L$^{\Delta T}$ mice and rested those cells in congenic WT recipient mice. At day 5, splenic CD4$^+$ T cells were enriched and assessed for their TCR signal strength. As expected, retrieved DOT1L-deficient CD4$^+$ T cells showed decreased CD5 expression compared with that of WT CD4$^+$ T cells and increased TCR signal strength as assessed by Nur77 and CD69 expression (Figures S1C–S1E), highlighting that DOT1L controls activation of peripheral CD4$^+$ T cells, likely through cell-intrinsic changes in TCR signaling that are independent of the lymphopenic conditions in the DOT1L$^{\Delta T}$ mice.

DOT1L Limits IFN-γ Expression in CD4$^+$ T Cells

Strong TCR signaling has been correlated with the preferential induction of Th1 cells, even in the presence of Th2-cell-promoting adjuvants (Constant et al., 1995; Hosken et al., 1995; van

(I) Histogram for CD5 expression of splenic CD4$^+$ T cells from DOT1L$^{FL/FL}$ and DOT1L$^{\Delta T}$ mice.
(J) Analysis of TCR signaling strength in splenic CD4$^+$ T cells from DOT1L$^{FL/FL}$ (black) and DOT1L$^{\Delta T}$ (red) mice: CD4$^+$ T cells were incubated with increasing concentrations of plate-bound αCD3 for 4 h and analyzed for their expression of Nur77. Representative plot (left) and quantification of Nur77 expression (right).
(K) Representative plot (left) and quantification (right) of CD69 expression. Quantitative analysis of CD69 expression of CD4$^+$ T cells as described in (J).
All plots and graphs are representative of at least two independent experiments with three mice per group. Error bars represent means ± SEM. *p ≤ 0.05, **p ≤ 0.01, ***p ≤ 0.001. ns, non-significant.

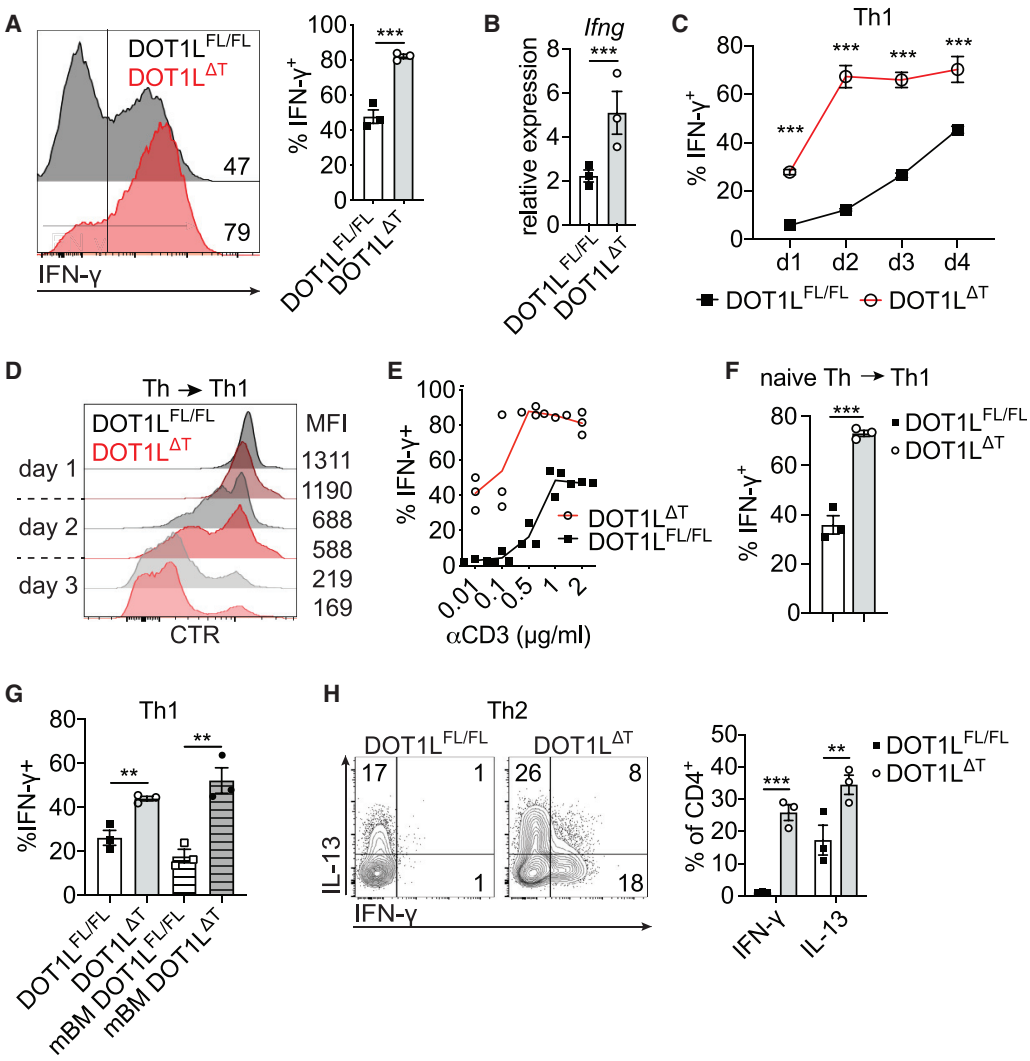

Figure 2. DOT1L Limits IFN-γ Expression in CD4⁺ T Cells

(A) Histogram of IFN-γ expression after culturing splenic CD4⁺ T cells from indicated mice under Th1-polarizing conditions. Numbers indicate %+ve (left). Quantification of individual mice from concatenated data in the histogram (right).

(B) *Ifng* expression analysis of mice in (A).

(C) Kinetics of IFN-γ expression under Th1-polarizing conditions of splenic CD4⁺ T cells of indicated mice.

(D) Kinetics of proliferative capacity of CD4⁺ T cells of indicated mice under Th1-polarizing conditions.

(E) IFN-γ expression with various stimulation of the TCR (plate-bound αCD3) under Th1-polarizing conditions.

(F) IFN-γ expression of splenic, FACS naive (CD44⁻ CD62L^{high}) CD4⁺ T cells under Th1-polarizing conditions for 3 days.

(G) IFN-γ expression of splenic CD4⁺ T cells from indicated mice and mixed bone marrow (mBM) chimeras under Th1-polarizing conditions.

(H) IFN-γ and IL-13 expression of splenic CD4⁺ T cells from indicated mice under Th2-polarizing conditions (left). Quantification of data on the left (right).

All plots and graphs are representative of at least two independent experiments with three mice per group. Error bars represent means ± SEM. **p ≤ 0.01, ***p ≤ 0.001.

Panhuys et al., 2014). As we previously reported, increased expression of IFN-γ after inhibition of DOT1L with a small-molecule inhibitor in *ex vivo* generated Th1 cells (Scheer et al., 2019) and based on the fact that CD4⁺ T cells show increased TCR signaling in the absence of DOT1L (Figure 1J), we analyzed whether CD4⁺ T cells from DOT1L^{ΔT} mice show increased expression of the Th1 cell signature cytokine IFN-γ. As expected, DOT1L-deficient Th cells showed significantly increased expression of IFN-γ under Th1-cell-polarizing conditions (Figures 2A and 2B), validating that depletion of DOT1L in CD4⁺ T cells has a similar effect to inhibiting DOT1L with the small-molecule inhibitor SGC0946 (Scheer et al., 2019). Interestingly, increased expression of IFN-γ in the absence of DOT1L under Th1-cell-polarizing conditions occurred rapidly after activation (Figure 2C), but that was not due to increased proliferation (Figure 2D). In line with a role for DOT1L in limiting TCR-induced activation, a 100-fold reduced concentration of αCD3 antibody led to expression of the same frequency of IFN-γ⁺ CD4⁺ T cells in the absence of

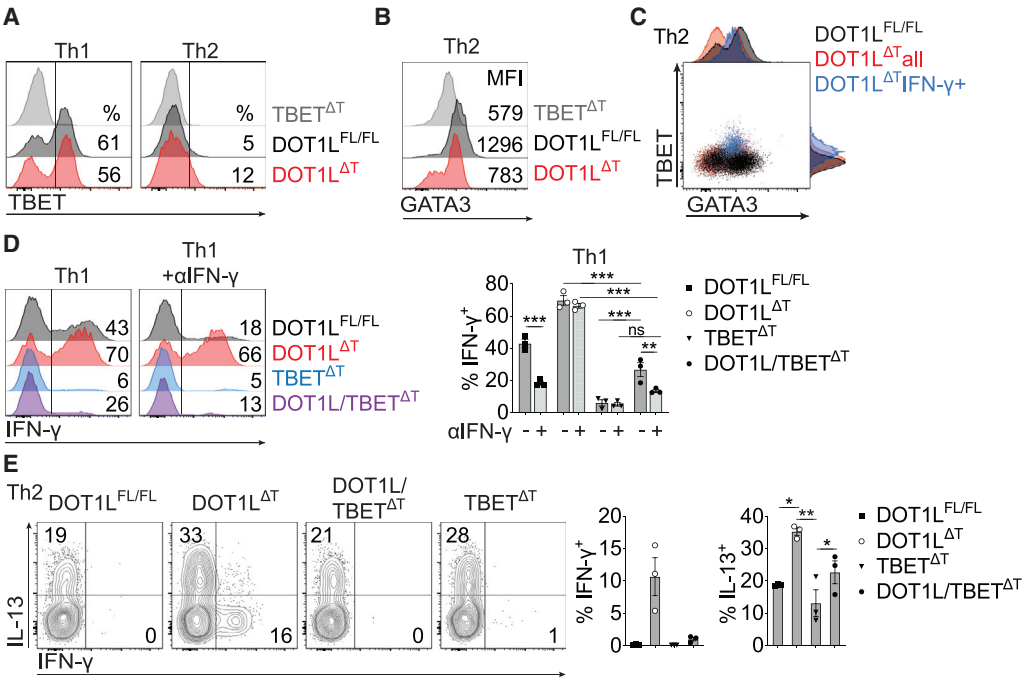

Figure 3. Dysregulated IFN-γ Production in DOT1L-Deficient Th Cells Is Largely Dependent upon TBET

(A) TBET expression of splenic CD4$^+$ T cells from indicated mice after culturing under Th1 or Th2 polarizing conditions.

(B) GATA3 expression of splenic CD4$^+$ T cells from indicated mice after culturing under Th2 polarizing conditions.

(C) TBET and GATA3 expression in CD4$^+$ T cells from indicated mice cultured under Th2-polarizing conditions. IFN-γ$^+$ CD4$^+$ T cells are highlighted in blue.

(D) IFN-γ expression of splenic CD4$^+$ T cells from indicated mice after culturing under Th1-polarizing conditions in the absence (Th1) or presence of neutralizing antibodies against IFN-γ (Th1 + αIFN-γ; left). Quantification of individual mice from one representative experiment (right).

(E) IL-13 and IFN-γ expression analysis of splenic CD4$^+$ T cells from indicated mice after culturing under Th2 polarizing conditions (left). Quantification of individual mice from one representative experiment (right).

Plots and graphs are representative of at least two independent experiments with three mice per group. Numbers in the plots indicate percentages. Error bars represent means ± SEM. *p ≤ 0.05, **p ≤ 0.01, ***p ≤ 0.001.

DOT1L compared with that of WT controls (Figure 2E). These results demonstrate that loss of DOT1L renders CD4$^+$ T cells hyper-sensitive to TCR signaling, resulting in increased IFN-γ production. To rule out biased identification of IFN-γ expression from mainly activated T cells, we polarized sorted splenic naive CD4$^+$ T cells (CD44$^-$ CD62L^{high}) under Th1-cell-polarizing conditions. As expected, DOT1L-deficient Th1 cells cultured from naive CD4$^+$ T cells also showed a similar phenotype of increased IFN-γ expression, proposing a cell intrinsic phenotype of increased IFN-γ expression of CD4$^+$ T cells in the absence of DOT1L (Figure 2F). Further, naive DOT1L-deficient CD4$^+$ T cells retrieved 5 days after being injected into non-lymphopenic WT mice displayed increased IFN-γ expression after culture under Th1-cell-polarizing conditions compared with that of recipient DOT1L-sufficient cells (Figure S2A). To rule out that the increased IFN-γ expression in the absence of DOT1L was a result from the lymphopenic environment during Th cell development, we generated mixed bone marrow chimeras (1:1 WT:DOT1L$^{\Delta T}$) and cultured splenic CD4$^+$ T cells under Th1-cell-polarizing conditions. The development of DOT1L-deficient CD4$^+$ T cells under non-lymphopenic conditions did not lead to normalized IFN-γ expression under Th1-cell-polarizing conditions (Figure 2G), demonstrating that the effects of DOT1L deletion are cell intrinsic. Interestingly, we also observed increased IFN-γ expression in CD4$^+$ T cells that were cultured under neutral conditions (Th0; Figure S2B). Strikingly, the absence of DOT1L in CD4$^+$ T cells also led to a highly significantly increase in expression of IFN-γ under Th2- and Th17-cell-polarizing conditions (Figures 2H and S2C), showing that DOT1L limits the sensitivity of TCR-dependent activation as well as lineage-specific and lineage-promiscuous expression of IFN-γ in effector Th cells.

Dysregulated IFN-γ Production in DOT1L-Deficient Th Cells Is Largely Dependent upon TBET

TBET is the signature transcription factor for Th1 cells, and upon induction, TBET stabilizes the Th1 cell gene program, resulting in increased expression of IFN-γ (Szabo et al., 2000, 2002). Because we observed increased expression of IFN-γ in the absence of DOT1L in Th0 (Figure S2B) and all effector Th cell lineages (Figures 2A 2G, and S2C) and because expression of TBET in Th2 cells leads to the production of IFN-γ (Szabo et al., 2000), we analyzed TBET expression in the absence of DOT1L in Th2 cells. In the absence of DOT1L, expression of TBET was not increased in Th1 cells and was slightly increased in Th2 cells (Figure 3A). As observed in CD4$^+$ T cells cultured under neutral conditions (Th0; Figure S3A), there was an associated reduction in expression of the master Th2 cell transcription factor GATA3 in DOT1L-deficient Th2 cells (Figure 3B). Strikingly, a

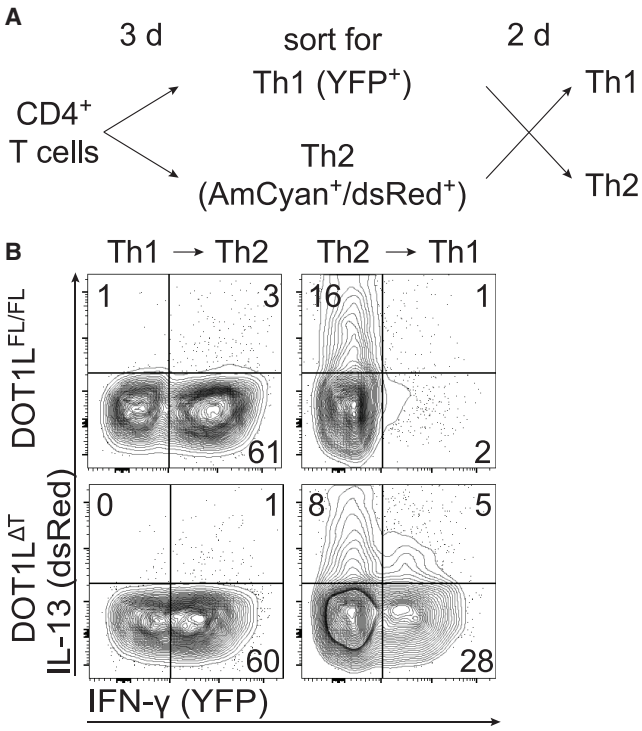

Figure 4. DOT1L Controls Th Cell Plasticity

(A) Experimental setup using control (DOT1L$^{FL/FL}$-IL-4-AmCyan/IL-13-dsRed/IFN-γ-YFP [CRY]) or DOT1L$^{\Delta T}$-CRY mice in (B).

(B) Th cells from indicated mice were cultured under Th1 or Th2 polarizing conditions for 3 days, FACS for bona fide Th1 (YFP$^+$) or bona fide Th2 (AmCyan$^+$/dsRed$^+$) cells and re-polarized under opposite conditions for 2 days.

Data shown is representative of two independent experiments (n = 3 mice per group, pooled after sort).

subset of DOT1L-deficient, GATA3^{low} Th2 cells showed increased expression of TBET, which also expressed IFN-γ (Figure 3C), showing that DOT1L not only regulates expression of IFN-γ but also regulates the lineage-promiscuous TBET expression in Th2 cells.

We next tested whether the increased expression of IFN-γ in the absence of DOT1L leads to enhanced IFN-γ expression through a feed-forward loop in Th cells. Treatment of WT Th1 cells with neutralizing antibodies against IFN-γ (αIFN-γ) resulted in a significant reduction in the expression of IFN-γ (Figure 3D, right). However, IFN-γ expression was not significantly reduced by neutralizing extracellular IFN-γ in the absence of DOT1L, highlighting that, in the absence of DOT1L, IFN-γ expression is independent of an IFN-γ feed-forward mechanism (Figure 3D). In line with that, a significant proportion of DOT1L-deficient Th2 cells expressed IFN-γ, despite being generated in the presence of αIFN-γ and in the absence of IL-12 (Figure 3E), identifying DOT1L as a critical, cell-intrinsic regulator of the Th1 cell differentiation program.

Because the αIFN-γ treatment failed to abolish IFN-γ production under both Th1- and Th2-cell-promoting conditions in the absence of DOT1L and IFN-γ expression seemed to be restricted to the TBET$^+$ population in Th2 cells (Figure 3C), we next analyzed whether TBET was required for expression of IFN-γ in those cells. To do that, we made use of T-cell-specific TBET and DOT1L/TBET double-knockout mice (TBET$^{\Delta T}$ and DOT1L/TBET$^{\Delta T}$ mice, respectively). Although TBET-deficient Th cells failed to differentiate into IFN-γ-producing Th1 cells, the additional absence of DOT1L allowed for moderate IFN-γ expression in the absence of TBET (Figures 3D and 3E). Interestingly, DOT1L-deficient CD4$^+$ T cells cultured under Th17-cell-polarizing conditions showed lineage-promiscuous expression of IFN-γ in the RORγt$^+$ population (Figures S3B and S3C), showing that DOT1L also limits IFN-γ expression in Th17 cells. Because we were unable to detect significant IFN-γ expression in CD4$^+$ T cells cultured under Th17-cell-polarizing conditions from DOT1L/TBET$^{\Delta T}$ mice (Figure S3B), we hypothesized that lineage-promiscuous IFN-γ expression in the absence of DOT1L in effector cells is dependent on TBET. Consistent with that finding in Th17 cells, the lineage-promiscuous expression of IFN-γ in Th2 cells was entirely dependent upon TBET, as DOT1L/TBET-deficient Th cells activated under Th2-cell-polarizing conditions failed to produce any detectable levels of IFN-γ (Figures 3D and 3E). Thus, the dysregulated production of IFN-γ in Th cells is TBET dependent, suggesting that DOT1L deficiency affects the upstream Th1 cell lineage-differentiation program, rather than controlling IFN-γ expression directly.

DOT1L Controls Th2 Cell Plasticity

Because we observed lineage-promiscuous expression of IFN-γ in the absence of DOT1L in Th2 and Th17 cells, we next tested whether DOT1L controls Th cell plasticity. The mechanism for lineage integrity between Th1 and Th2 cells has been best characterized among the Th cell lineages, showing mutually exclusive phenotypes (Mullen et al., 2001; Ouyang et al., 1998). Because Th1 and Th2 cells showed increased expression of the Th1 cytokine IFN-γ in the absence of DOT1L, we investigated the role of DOT1L for lineage integrity between Th1 and Th2 cells, as previously described (Allan et al., 2012; Tumes et al., 2013). Here, we made use of IL-4/IL-13/IFN-γ triple-reporter mice (IL-4-AmCyan/IL-13-dsRed/IFN-γ-YFP; CRY mice (Huang et al., 2015; Reinhardt et al., 2009). These mice allowed us to distinguish between committed Th1 (YFP$^+$) or Th2 (AmCyan$^+$/dsRed$^+$) cells and uncommitted but activated cells after primary Th1- or Th2-cell-polarizing conditions (Figure 4A). Committed Th1 (YFP$^+$) and Th2 (AmCyan$^+$/dsRed$^+$) cells generated from DOT1L-sufficient mice were stable, with <4% of cells switching after reactivation (Figure 4B, top). We did observe a significant proportion of cells that did not express either cytokine upon repolarization. However, DOT1L-sufficient Th1 and Th2 cells did not produce lineage-promiscuous cytokines after re-polarization, demonstrating lineage integrity. Interestingly, DOT1L-deficient Th1 cells were also highly stable and failed to express IL-13 under Th2-cell-inducing conditions. This suggests that loss of DOT1L has no effect on the switching of committed Th1 cells and that DOT1L is dispensable for Th1 cell lineage stability. In contrast, a significant frequency (>30%) of DOT1L-deficient Th2 (AmCyan$^+$/dsRed$^+$) cells stimulated under secondary Th1-cell-polarizing conditions produced IFN-γ (YFP$^+$), showing that

CellPress
OPEN ACCESS

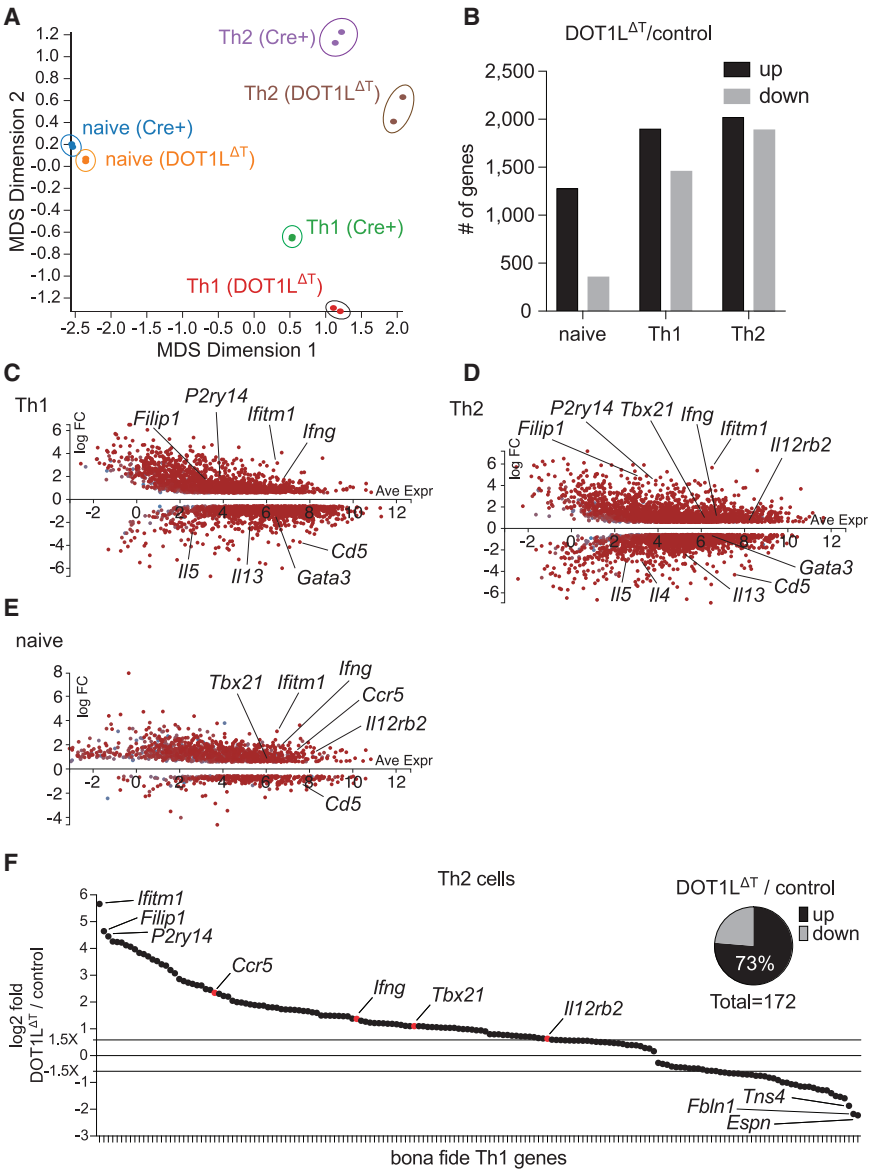

Figure 5. DOT1L Limits Th1-Cell-Associated Gene Expression

(A) Principal-coordinate analysis (PCA) of RNA-sequencing (Table S1) from naive (CD44^{-} CD62L^{high}) Th, bona fide Th1, and Th2 cells from control (Cre^{+}) and DOT1L$^{\Delta T}$ mice.

(B) Number of up- and downregulated genes from RNA-seq analysis (FDR cutoff, 0.05; absolute log-fold > 0.585 = > 1.5-fold) of indicated cells.

(C–E) MA plots for differentially expressed genes, see (B), in the absence of DOT1L in bona fide Th1 (C), Th2 (D), and naive (E) Th cells.

(F) Signature Th1 genes (Stubbington et al., 2015) that overlap with differentially expressed genes in the absence of DOT1L (DOT1L$^{\Delta T}$/control) in Th2 cells.

Data shown are from one experiment (n = 2).

DOT1L is critically required to control committed Th2 cell plasticity by inhibiting IFN-γ expression (Figure 4B).

DOT1L Limits Th1-Cell-Associated Gene Expression

After establishing that DOT1L promotes lineage integrity, we aimed to identify the role of DOT1L as a negative regulator of the Th1-cell-associated gene program. We, therefore, performed genome-wide expression analysis by RNA sequencing (RNA-seq) to understand the role of DOT1L-dependent H3K79me2 for specific gene expression in Th cells. Principal-coordinate analysis (PCA) showed high similarities between the two biological replicates of each, naive Th, Th1, and Th2 samples from DOT1L$^{\Delta T}$ mice or *Cd4*-Cre^{+} controls. Further, PCA shows that DOT1L-deficient Th2 cells are more similar to Th1 cells compared to DOT1L-sufficient Th2 cells, indicating a shift toward a Th1 cell program in Th2 cells from DOT1L$^{\Delta T}$ mice (Figure 5A). Analysis of the number of up- and downregulated genes in Th cell subsets showed an increased number of genes with higher expression in DOT1L-deficient Th cells (Figure 5B; Table S1), suggesting a potential inhibitory role for DOT1L in regulation of gene expression. MA plots of significantly dysregulated genes (Th1/*Cd4*-Cre^{+} or Th2/*Cd4*-Cre^{+}; false-discovery rate [FDR] cutoff, 0.05; absolute log-fold > 0.585 = > 1.5-fold expression) in the absence of DOT1L show similar Th1 cell differentiation program-associated upregulated genes in Th1 and Th2 polarized cells (Figures 5C and 5D), which was already partially manifested in the unpolarized, naive state of the cells (Figure 5E). We further compared the results from our RNA-seq for Th2 polarized cells with published data on a set of bona fide Th1-cell-associated genes (Stubbington et al., 2015). Strikingly, we found that 73% of all the Th1-cell-specific genes were significantly increased in DOT1L-deficient Th2 cells (Figure 5F), further highlighting that DOT1L deficiency is associated with significant upregulation of the Th1 cell gene program.

DOT1L-Dependent H3K79me2 Is Associated with Lineage-Specific Gene Expression

Our results show that loss of DOT1L leads to the increased expression of IFN-γ and an increased Th1 cell gene program in Th cells. However, the role of DOT1L-dependent H3K79me2 in Th cells is unclear. Therefore, we next made use of CRY mice to analyze the distribution of H3K79me2 in naive or cultured and fluorescence-activated cell sorted (FACS) bona fide Th1 (YFP^{+}) or bona fide Th2 (AmCyan^{+}/dsRed^{+}) cells across the genome. PCA of three biological replicates showed high consistency within the samples of Th cell subsets and high diversity between groups (Figure S4A). H3K79me2 plot profiles of all genes ±10 Kb upstream of

the transcriptional start site (TSS) and ±10 Kb downstream of the transcriptional end site (TES) revealed increased coverage of H3K79me2 in all Th cell subsets in the body of genes. Overall levels of H3K79me2 were increased in Th1 and Th2 cells compared with naive Th cells (Figure S4B), suggesting increased H3K79me2 coverage for genes in activated Th cells.

In general, H3K79me2 levels were high in all Th cell subsets at lineage-specific, and low at non-Th lineage-specific, genes, such as for *Cd4* and *Myod1* (Figure 6A), respectively. Increased coverage at the genes for *Ifng* and *Tbx21* in Th1 cells (Figure 6B), and *Il13* and *Gata3* in Th2 cells (Figure 6C) suggests that H3K79me2 is primarily correlated with active Th cell lineage-specific gene expression.

DOT1L-Dependent H3K79me2 Is Associated with a Subset of Highly Expressed Genes

Our data suggest a correlation of H3K79me2 coverage with lineage-specific gene expression. Although signal strength of H3K79me2 was previously correlated with gene expression in mixed-lineage leukemia (MLL)-rearranged leukemia (Bernt et al., 2011), the correlation between H3K79me2 coverage and gene expression in Th cells is unknown. To unveil the dependence of H3K79me2 for gene expression in Th cells, we clustered genes from each Th cell subset by gene expression into low (<20 counts), mid (~500 counts), or high (top 450 expressed genes) and assessed the coverage of H3K79me2 ± 3 Kb around the TSS. Analysis of the clusters revealed that the strength of the gene expression correlated with the coverage for H3K79me2, with highly expressed genes showing the greatest average H3K79me2 coverage and little coverage for low-expressed genes (Figure 6D). However, analysis of each individual highly expressed gene for its presence of H3K79me2 revealed high heterogeneity with regard to H3K79me2 coverage: although some highly expressed genes are also highly enriched for H3K79me2 (subcluster "a"), other highly expressed genes show little to no enrichment for H3K79me2 (subcluster "b") (Figure 6E, high gene expression), or subclusters "c" and "d" in the intermediary expressed genes (Figure 6E, mid gene expression). The cluster of low gene expression did not show a significant heterogeneity (Figure 6E, low gene expression). We, therefore, analyzed the genes in subclusters a, b, c, and d for their expression in the absence of DOT1L, comparing gene expression between naive Th cells from DOT1L$^{FL/FL}$ and DOT1L$^{\Delta T}$ mice. Although genes in subcluster a showed highly significantly reduced expression in the absence of DOT1L, genes in subcluster b–d showed moderately, non-significant, reduced expression in the absence of DOT1L (Figure 6F), suggesting that DOT1L-dependent H3K79me2 is specifically required for maintaining the expression of a subset of highly expressed genes.

Because we observed increased gene expression in the presence of H3K79me2 across the genome and an increased Th1 cell differentiation program in the absence of DOT1L, we could either argue that H3K79me2 is an inhibitory mark or that genes inhibiting the Th1 program are less expressed in the absence of DOT1L and H3K79me2. The latter hypothesis is more likely because we and others observed that methylation of H3K79 by DOT1L is primarily associated with transcriptional activity (Bernt et al., 2011; Cattaneo et al., 2016). Together with our data suggesting that DOT1L deficiency affects the upstream Th1 cell lineage differentiation program, rather than directly controlling IFN-γ expression (Figure 3), we, therefore, focused on the identification of master regulator genes with decreased gene expression in DOT1L-deficient CD4$^+$ T cells. We identified 15 TFs that were significantly downregulated across all Th cell subsets in the absence of DOT1L; seven of which are known to inhibit the Th1 cell differentiation program (red), five of which have not been defined with regard to their influence of the Th1 cell differentiation program (black), and three of which promote the Th1 cell differentiation program (green). Most prominently, the TFs BACH2, FOXP3, and NR4A3 were among the highest downregulated TFs across naive Th, Th1, and Th2 cells in the absence of DOT1L compared with DOT1L-sufficient cells (Figure 6G); all of which have been correlated to limiting the Th1 cell differentiation program (Edwards et al., 2018; Sekiya et al., 2011; Yang et al., 2017). As an example, the Th1 program-inhibiting TF BACH2 was one of the highest downregulated TFs across all Th cell subsets and clustered within the highest H3K79me2-covered genes (Figure 6H), suggesting a role for DOT1L and H3K79me2 in maintaining its gene expression across Th cell subsets and thereby limiting the Th1 cell differentiation program. In line with the downregulation of BACH2 expression in the absence of DOT1L, chromatin immunoprecipitation (ChIP)-qPCR of the *Bach2* locus shows reduced coverage of H3K79me2 in mesenteric lymph-node-derived (low-dose *Trichuris muris* infection model) Th1 (YFP$^+$) cells from DOT1L$^{\Delta T}$ mice. Further, coverage of H3K79me2 was also reduced at the *Ifng* locus in these mice, thus showing that DOT1L appears to control Th cell differentiation and gene expression through both direct and indirect mechanisms.

DOT1L Limits the Th1 Program during Helminth Infection

Our results demonstrate that DOT1L is critical for limiting the Th1 cell program and expression of IFN-γ in all Th cell subsets. To identify the role of DOT1L in CD4$^+$ T cells for infection, we made use of the *Trichuris muris* infection model. In that model, a high-dose infection (~200 eggs) of C57BL/6J mice results in the development of a protective Th2-cell-biased immune response, associated with goblet cell hyperplasia and mucus production, ultimately leading to worm expulsion. However, if the immune response in the infected mice shows an increased type 1 response, those mice will not expel *Trichuris* and will become chronically infected (Bancroft et al., 1997, Bancroft et al., 2001).

To test whether DOT1L orchestrates immunity to *T. muris* infection, we infected DOT1L$^{FL/FL}$ and DOT1L$^{\Delta T}$ mice with 200 eggs. After infection, DOT1L$^{\Delta T}$ mice maintained a significant worm burden at day 21 post-infection (Figure 7A) and developed a non-protective Th1 cell response, with high levels of IFN-γ, low levels of IL-13 and IL-4 (Figures 7B, 7C, and S5A), and lower IL-4 expression (Figure S5E). As expected, we also observed reduced levels of *Trichuris*-specific immunoglobulin G1 (IgG1) (Figure 7D). We did not detect decreased frequencies of T follicular helper (Tfh) cells among the CD4$^+$ T cell population (Figure S5B) or their capacity to produce IL-4 (Figure S5C) in *Trichuris*-infected mice. However, because the numbers of CD4$^+$ T cells in DOT1L$^{\Delta T}$ mice were significantly decreased, the overall reduced numbers of Tfh cells (Figure S5D) likely contributed to the lower levels of IL-4 and the non-protective phenotype

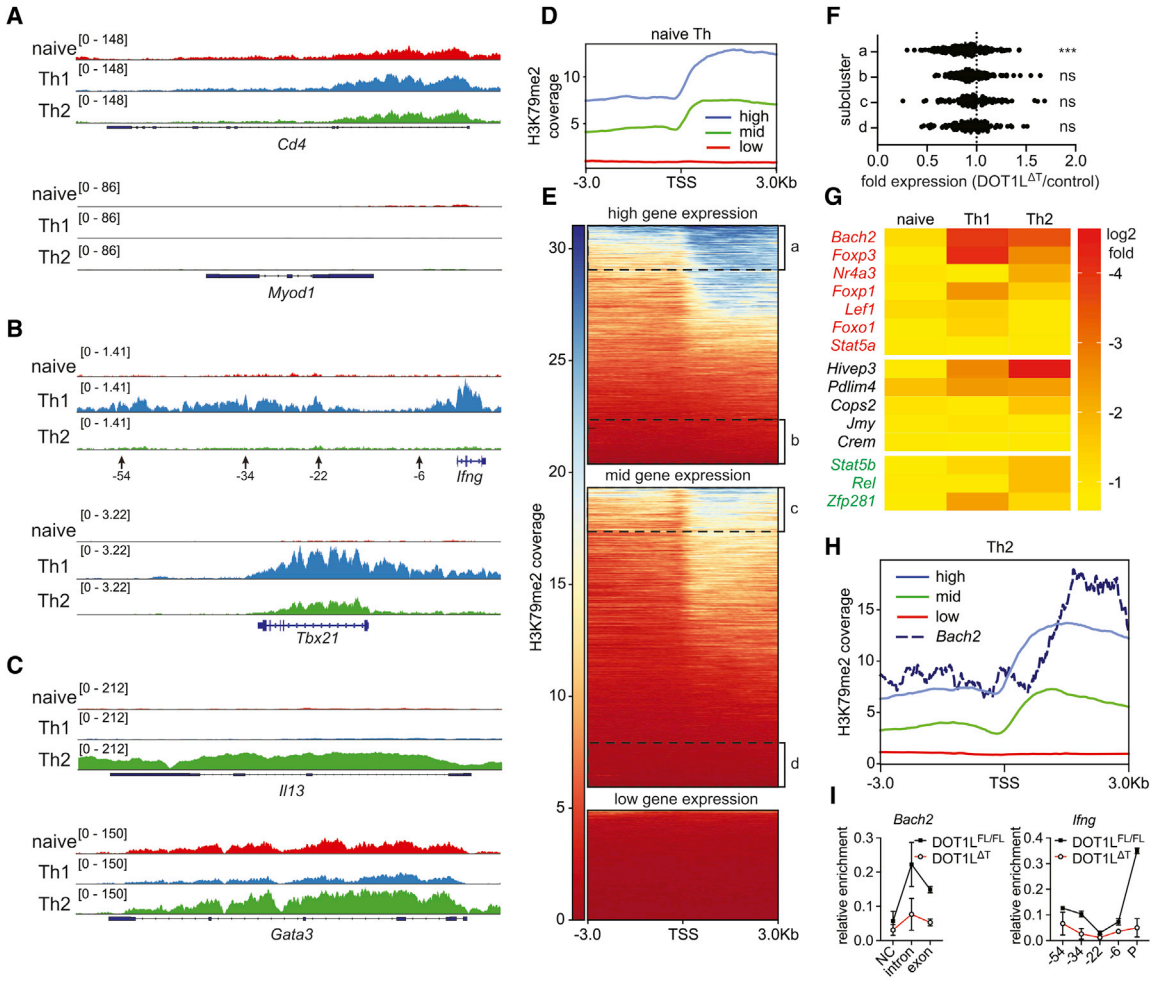

Figure 6. DOT1L-Dependent H3K79me2 Is Associated with Lineage-Specific Genes

(A–C) H3K79me2 coverage at the indicated genes.

(A) T cell lineage-specific *Cd4* gene locus and lineage-unspecific gene locus of *Myod1*.

(B) Th1-cell-specific *Ifng* locus and depicted regulatory regions upstream and *Tbx21* locus.

(C) Th2-cell-specific gene loci *Il13* and *Gata3*. Data shown are from one H3K79me2 ChIP-seq experiment with three biological replicates and are visualized with deepTools plotProfile or the Integrative Genomics Viewer (IGV).

(D) Coverage of H3K79me2 ± 3 Kb around the TSS in wild-type, naive Th cells grouped by expression strength: low (<20 counts), mid (~500 counts), and high (top 450 expressed genes).

(E) Heatmap of H3K79me2 coverage ±3 Kb around the TSS, clustered in high-, mid-, and low-expressed genes. Subclusters a and b comprise of the top and bottom 1,000 peaks (a, 185 different genes; b, 143 different genes) for highly expressed genes, and subclusters c and d comprise the 100 top and 100 bottom genes of the intermediary expressed genes, regarding H3K79me2 coverage scores.

(F) Fold expression of genes in subclusters a, b, c, and d (Figure 6B, high and mid gene expression) in the presence or absence of DOT1L in naive Th cells.

(G) Transcription factors (from RNA-seq experiment; Figure 5; Table S1) that were downregulated across all Th cell subsets (naive Th, Th1, and Th2) in the absence of DOT1L compared with control mice. Red indicates genes that inhibit the Th1 cell differentiation program, black shows unknown genes with regard to regulation of the Th1 cell differentiation program, and green represents genes that promote the Th1 cell differentiation program.

(H) Coverage of H3K79me2 ±3 Kb around the TSS in Th2 cells, grouped by expression strength: low (< 0 counts), mid (~500 counts), and high (top 450 expressed genes), and the coverage of H3K79me2 at the TSS of *Bach2*. Data were visualized using deepTools (Ramírez et al., 2016).

(I) H3K79me2 ChIP-qPCR of *in vivo* generated bona fide Th1 cells (three mice pooled per sample; n = 2) at indicated sites. NC, negative control (see Figure S4C). Data shown are representative of one experiment (n = 2–3). Statistical significance to the unchanged ratio in gene expression (x = 1) was determined by one-way ANOVA. ***p ≤ 0.001. ns, non-significant.

observed in DOT1L$^{\Delta T}$ mice. Further, treatment of mice with monoclonal antibodies against IFN-γ (αIFN-γ) failed to reduce the levels of IFN-γ or increase the IL-4 expression in the proximal colon (Figure S5E), thereby failing to promote resistance to infection in the absence of DOT1L (Figures 7A–7E). This suggests that neutralizing IFN-γ alone is not sufficient to overcome the increased IFN-γ/Th2 cytokine ratio needed to expel the worms. Therefore, consistent with our *in vitro* results, DOT1L appears to be a T-cell-intrinsic factor that is critical for limiting the development of a Th1 cell response during helminth infection *in vivo*.

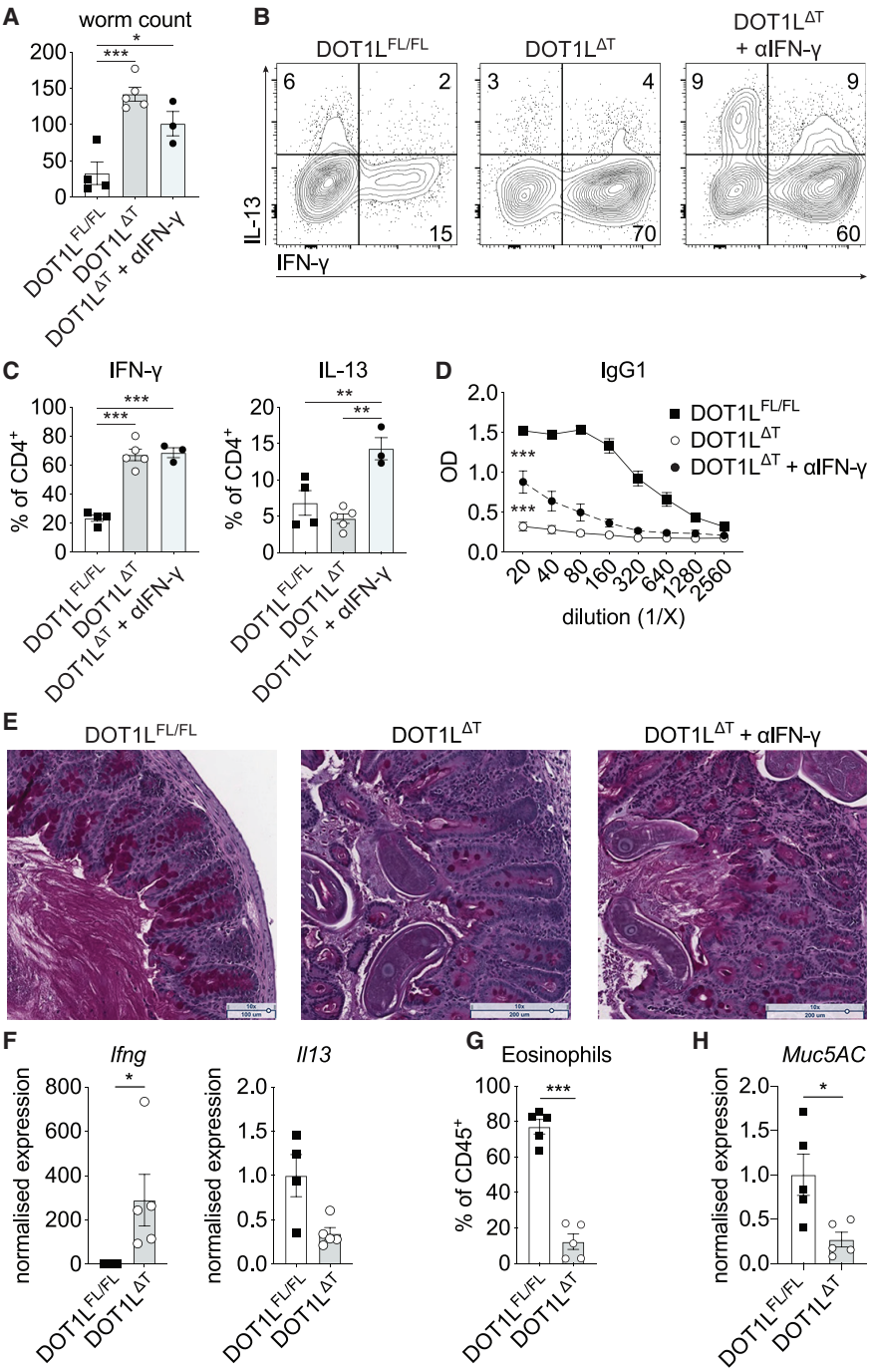

Figure 7. DOT1L Limits the Th1 Program during Infection and Immunity

(A) Worm count in the cecum 21 days after infection of control (DOT1L$^{FL/FL}$) or DOT1L$^{\Delta T}$ mice with 200 eggs of *Trichuris muris*. Where indicated, some DOT1L$^{\Delta T}$ mice were additionally treated with neutralizing antibodies against IFN-γ.

(B) Production of IFN-γ and IL-13 from mesenteric lymph node cells (gated on viable CD4$^+$ T cells) 3 days after restimulation with αCD3 and αCD28 *ex vivo*.

(C) Quantification of (B).

(D) *T. muris*-specific serum IgG1 from the same mice as (A).

(E) Histology (PAS stain) of cecum tips from representative mice in (A).

(F–H) qPCR analysis of the indicated genes from whole lung tissue from mice sensitized and challenged with house dust mite (HDM) allergen.

(G) Eosinophils in the bronchoalveolar lavage from mice in (F).

(H) qPCR analysis of the lungs for *Muc5AC*.

Data shown are representative of two independent experiments (n = 4–5 mice per group). Statistical significance was determined with a two-tailed Student's t test (F, G, and H) or one-way ANOVA (A, C, and D). Error bars represent means ± SEM. *p ≤ 0.05, **p ≤ 0.01, ***p ≤ 0.001.

T-Cell-Intrinsic Expression of DOT1L Is Required for Th2-Cell-Dependent Inflammation

To further validate that DOT1L is critical for limiting the Th1 cell program and expression of IFN-γ *in vivo*, we treated DOT1L$^{FL/FL}$ or DOT1L$^{\Delta T}$ mice intranasally with house dust mite (HDM) antigen. In C57BL/6 mice, HDM induces a cascade of type 2 immune responses, including group 2 innate lymphoid cells and Th2 cells, culminating with the recruitment of eosinophils into the lungs (Hoyne et al., 1993). Consistent with our findings *in vitro* and during helminth infection, loss of DOT1L in T cells during allergic lung inflammation resulted in an increase in IFN-γ expression and reduced levels of IL-13 (Figure 7F). This led to significantly fewer eosinophils (CD45$^+$ SiglecF$^+$ CD11c^{neg}; Figure 7G) in the lungs and significantly decreased expression of *Muc5AC*, a marker of mucous production in the lungs of DOT1L$^{\Delta T}$ mice (Figure 7H). These results suggest that targeting DOT1L could provide a therapeutic strategy to limit pathogenic Th2 cell responses.

In summary, the experiments described here provide evidence of a pivotal role for DOT1L and H3K79me2 in limiting the Th1 cell program and the production of IFN-γ, which has a significant effect on immunity to infection and the development of inflammation. These findings place DOT1L as a central regulator of the Th1 cell gene program and identify this pathway as a potential therapeutic target to treat diseases associated with dysregulated Th cell responses.

DISCUSSION

KMTs are a fundamental part of the epigenetic machinery that can influence the outcome of the Th-cell-mediated immune response. As such, the KMTs G9a, EZH2, or SUV39H1 have previously been shown to be important factors in Th cell

differentiation and Th-cell-dependent immune response in infection and inflammation (Allan et al., 2012; Antignano et al., 2014; Lehnertz et al., 2010; Tumes et al., 2013). In the present study, we identify a central role for DOT1L in limiting $CD4^+$ T cell activation, the production of IFN-γ in Th1 cells, and the lineage-promiscuous production of IFN-γ in effector T cell lineages during protective and pathogenic inflammatory responses.

The role of DOT1L is best described in the setting of cancer (Bernt et al., 2011; Wang et al., 2019). However, we previously identified DOT1L as a key player in the immune system by limiting IFN-γ in Th1 cells using the specific small-molecule inhibitor SGC0946 (Scheer et al., 2019). Based on these data, we generated conditional T-cell-specific DOT1L knockout mice ($DOT1L^{\Delta T}$) to identify its role *in vivo*. Although $DOT1L^{\Delta T}$ mice are healthy and fertile, they showed T cell lymphopenia and an activated phenotype of Th cells in the periphery. This activated phenotype was similar to CD4Cre/R-DTA mice that show peripheral T cell lymphopenia (Voehringer et al., 2008). However, activation of $CD4^+$ T cells in the absence of DOT1L was independent of increased proliferation in the periphery. Our transfer and bone marrow chimera experiments further showed that the increased IFN-γ production by activated $CD4^+$ T cells in the absence of DOT1L was cell intrinsic and not dependent on the T cell lymphopenic conditions. Despite high levels of CD44 in the absence of DOT1L and reports that high CD44 expression leads to a Th17 phenotype (Schumann et al., 2015), $CD4^+$ T cells in the absence of DOT1L produced increased IFN-γ over IL-17. Because we observed decreased expression of CD5 and increased expression of Nur77 and CD69 in the absence of DOT1L as markers of TCR activation, our finding of a Th1-biased development of $CD4^+$ T cells is consistent with reports that stronger TCR signaling is correlated to induction of Th1 cells, even in the presence of Th2-promoting conditions (Constant et al., 1995; Hosken et al., 1995; van Panhuys et al., 2014).

Lineage-promiscuous expression of IFN-γ in Th2 cells was also previously found in the absence of the KMTs EZH2 (Tumes et al., 2013) and SUV39H1 (Allan et al., 2012), demonstrating that production of IFN-γ is a tightly regulated process. Indeed, both EZH2 and SUV39H1 have been shown to regulate TBET expression in Th2 cells, leading to lineage-promiscuous IFN-γ expression. However, DOT1L deficiency is unique in that neither EZH2 nor SUV39H1/2 was shown to limit activation of $CD4^+$ T cells or that their absence leads to T cell lymphopenia. In addition, neither $EZH2^{\Delta T}$ nor $Suv39H1^{\Delta T}$ mice showed the thymic phenotype of increased cell death of CD4SP cells of $DOT1L^{\Delta T}$ mice, supporting DOT1L's unique role in limiting activation and peripheral T cell survival among analyzed KMTs in T cell biology.

Expression of IL-13 is cooperatively regulated by c-Myb and GATA3. Indeed, we observe reduced expression of GATA3 under Th2 polarizing conditions in the absence of DOT1L, yet highly increased expression of c-Myb in the absence of DOT1L (Table S1). We may, therefore, observe increased expression of IL-13 because increased c-Myb proteins can recruit the remaining GATA3 to increase expression of IL-13 (Kozuka et al., 2011). Reduced expression of this master TF for Th2 cells in naive cells could also be the reason for the increased Th1 phenotype in the absence of DOT1L, thereby failing to develop into fully competent Th2 cells. However, we also observed increased IFN-γ and IL-17 expression in Th17 cells, which are not dependent on GATA3, which argues against a direct involvement of GATA3 in inhibiting the lineage-promiscuous IFN-γ expression in effector Th cells in the absence of DOT1L.

Our finding that DOT1L-dependent H3K79me2 is associated with a subset of highly expressed genes is consistent with several previous studies that correlate the presence of H3K79me2 with gene expression and transcriptional elongation (Chen et al., 2020; Guenther et al., 2007; Im et al., 2003; Kryczek et al., 2014; Pursani et al., 2018; Steger et al., 2008; Wang et al., 2008). Despite our own findings and previous reports that correlate DOT1L-dependent H3K79me2 with gene expression (Bernt et al., 2011; Steger et al., 2008), H3K79me2 is not necessarily required for gene expression. Based on our gene-expression data and H3K79me2 coverage analysis, we suggest that a subset of highly expressed genes is dependent on the presence of H3K79me2. Although the reason why some genes are dependent on the presence of H3K79me2 and others are not is the subject of ongoing investigations (Kwesi-Maliepaard et al., 2020). In the absence of DOT1L, some genes are significantly downregulated across Th cell subsets in the absence of H3K79me2. Among those genes are the Th1 cell differentiation program-inhibiting TFs BACH2, NR4A3, and FOXO1 (Edwards et al., 2018; Kerdiles et al., 2010; Sekiya et al., 2011). For example, BACH2 has been described as a potent and central regulator of the Th cell differentiation program, suppressing lineage-promiscuous IFN-γ expression in $CD4^+$ T cells under Th1-, Th2-, and Th17-polarizing conditions, showing a highly similar phenotype when compared with the loss of DOT1L (Edwards et al., 2018; Kim et al., 2014; Roychoudhuri et al., 2013).

We found that the T-cell-intrinsic expression of DOT1L was required to restrain Th1 cell lineage during immunity and inflammation *in vivo*. After infection with the helminth parasite *Trichuris*, $DOT1L^{\Delta T}$ mice failed to develop a protective Th2 cell response (Else and Grencis, 1996) and were susceptible to infection, despite the ability to induce Tfh cells in the absence of DOT1L. Treatment of mice with αIFN-γ slightly increased the production of type-2-associated factors, such as IL-13, IgG1, and mucus, but failed to induce immunity to infection, further highlighting the T-cell-intrinsic role for DOT1L to limit Th1 cell differentiation. This phenotype is similar to that of mice with a T-cell-specific deletion of the KMT G9a because both mice fail to mount an efficient Th2 immune response, which is needed to expel *Trichuris* (Else and Grencis, 1996; Lehnertz et al., 2010). However, unlike DOT1L-deficient Th cells, G9a-deficient Th cells do not show increased production of IFN-γ under Th2-polarizing conditions, highlighting that distinct epigenetic mechanisms operate to control Th cell differentiation and function. However, both *in vivo* models herein clearly specify a skewed Th1 immune response, showing that DOT1L limits the production of IFN-γ and the Th1 program *in vivo*.

Our data show that inhibition of DOT1L may be a highly efficient way of treating Th2-dependent inflammation, e.g., in patients with asthma that show an increased Th2/Th1 ratio. DOT1L is an especially interesting target because the small-molecule inhibitor pinometostat is currently approved for use in patients with MLL-rearranged (MLL*r*) leukemia (Stein et al., 2015, 2018), which offers the possibility of repurposing this

drug for other diseases. Interestingly, to date, there are no reports, to our knowledge, on the effects of pinometostat on other cells in patients with MLL*r* leukemia, especially with regard to their IFN-γ production. This highlights the need for further studies in these patients with regard to Th cell differentiation and cytokine production and accentuates the possibility that changes in T cell biology may account for the effect of pinometostat in these patients.

Taken together, we show that DOT1L is a central regulator of Th cell differentiation and function and identify DOT1L as a potential therapeutic target to treat diseases associated with dysregulated type 2 immunity.

STAR★METHODS

Detailed methods are provided in the online version of this paper and include the following:

- KEY RESOURCES TABLE
- RESOURCE AVAILABILITY
  - Lead contact
  - Materials availability
  - Data and code availability
- EXPERIMENTAL MODEL AND SUBJECT DETAILS
- METHOD DETAILS
  - Mixed bone marrow chimeras
  - House dust mite (HDM) model of allergic asthma
  - Trichuris muris infection
  - T cell assays
  - Western blot
  - ELISA
  - RNA-sequencing
  - Expression analysis
  - Chromatin Immunoprecipitation (ChIP)
  - ChIP-sequencing
  - ChIP-qPCR
- QUANTIFICATION AND STATISTICAL ANALYSIS

SUPPLEMENTAL INFORMATION

Supplemental Information can be found online at https://doi.org/10.1016/j.celrep.2020.108505.

ACKNOWLEDGMENTS

We would like to thank Dr. Kim Jacobson for constructive comments and advice on the manuscript. We thank the Monash animal facility, Micromon; the Monash Flow Core facility; and the Monash Bioinformatics platform for their excellent technical support and assistance. We thank Dr. Ron Germain (NIAID) and Dr. Simon Phipps (QIMR Berghofer) for providing 4C13R mice (Huang et al., 2015). This work was supported by NHMRC project grants (APP1104433 and APP1104466) and a Monash platform access grant (PAG19-0642). Graphical Abstract was created using BioRender.com.

AUTHOR CONTRIBUTIONS

Conceptualization, S.S., B.R., and C.Z.; Methodology, S.S. and C.Z.; Investigation, M.B., J.R., A.Z., J.E., G.R., and J.N.; Writing – Original Draft, S.S. and C.Z.; Writing – Review & Editing, S.S. and C.Z.; Funding Acquisition, C.Z. and S.S.; Supervision, S.S., M.B., and C.Z.; Visualization, S.S. and J.R.; Formal Analysis, S.S.; Validation, J.R., M.B., J.E., and S.S.

DECLARATION OF INTERESTS

The authors declare no competing interests.

Received: July 15, 2020
Revised: October 5, 2020
Accepted: November 17, 2020
Published: December 15, 2020

REFERENCES

Allan, R.S., Zueva, E., Cammas, F., Schreiber, H.A., Masson, V., Belz, G.T., Roche, D., Maison, C., Quivy, J.-P., Almouzni, G., and Amigorena, S. (2012). An epigenetic silencing pathway controlling T helper 2 cell lineage commitment. Nature *487*, 249–253.

Antignano, F., Burrows, K., Hughes, M.R., Han, J.M., Kron, K.J., Penrod, N.M., Oudhoff, M.J., Wang, S.K.H., Min, P.H., Gold, M.J., et al. (2014). Methyltransferase G9A regulates T cell differentiation during murine intestinal inflammation. J. Clin. Invest. *124*, 1945–1955.

Antignano, F., Mullaly, S.C., Burrows, K., and Zaph, C. (2011). *Trichuris muris* infection: a model of type 2 immunity and inflammation in the gut. J. Vis. Exp. *51*, e2774.

Ashouri, J.F., and Weiss, A. (2017). Endogenous Nur77 is a specific indicator of antigen receptor signaling in human T and B cells. J. Immunol. *198*, 657–668.

Bancroft, A.J., Else, K.J., Humphreys, N.E., and Grencis, R.K. (2001). The effect of challenge and trickle *Trichuris muris* infections on the polarisation of the immune response. Int. J. Parasitol. *31*, 1627–1637.

Bancroft, A.J., Else, K.J., Sypek, J.P., and Grencis, R.K. (1997). Interleukin-12 promotes a chronic intestinal nematode infection. Eur. J. Immunol. *27*, 866–870.

Bernt, K.M., Zhu, N., Sinha, A.U., Vempati, S., Faber, J., Krivtsov, A.V., Feng, Z., Punt, N., Daigle, A., Bullinger, L., et al. (2011). MLL-rearranged leukemia is dependent on aberrant H3K79 methylation by DOT1L. Cancer Cell *20*, 66–78.

Cattaneo, P., Kunderfranco, P., Greco, C., Guffanti, A., Stirparo, G.G., Rusconi, F., Rizzi, R., Di Pasquale, E., Locatelli, S.L., Latronico, M.V.G., et al. (2016). DOT1L-mediated H3K79me2 modification critically regulates gene expression during cardiomyocyte differentiation. Cell Death Differ. *23*, 555–564.

Chen, X., Liu, X., Zhang, Y., Huai, W., Zhou, Q., Xu, S., Chen, X., Li, N., and Cao, X. (2020). Methyltransferase Dot1l preferentially promotes innate IL-6 and IFN-β production by mediating H3K79me2/3 methylation in macrophages. Cell. Mol. Immunol. *17*, 76–84.

Chenery, A.L., Antignano, F., Burrows, K., Scheer, S., Perona-Wright, G., and Zaph, C. (2015). Low-dose intestinal *Trichuris muris* infection alters the lung immune microenvironment and can suppress allergic airway inflammation. Infect. Immun. *84*, 491–501.

Constant, S., Pfeiffer, C., Woodard, A., Pasqualini, T., and Bottomly, K. (1995). Extent of T cell receptor ligation can determine the functional differentiation of naive $CD4^+$ T cells. J. Exp. Med. *182*, 1591–1596.

Edwards, C.L., de Oca, M.M., de Labastida Rivera, F., Kumar, R., Ng, S.S., Wang, Y., Amante, F.H., Kometani, K., Kurosaki, T., Sidwell, T., et al. (2018). The Role of BACH2 in T cells in experimental malaria caused by *Plasmodium chabaudi chabaudi* AS. Front. Immunol. *9*, 2578.

Else, K.J., and Grencis, R.K. (1996). Antibody-independent effector mechanisms in resistance to the intestinal nematode parasite *Trichuris muris*. Infect. Immun. *64*, 2950–2954.

Frederiks, F., Tzouros, M., Oudgenoeg, G., van Welsem, T., Fornerod, M., Krijgsveld, J., and van Leeuwen, F. (2008). Nonprocessive methylation by Dot1 leads to functional redundancy of histone H3K79 methylation states. Nat. Struct. Mol. Biol. *15*, 550–557.

Guenther, M.G., Levine, S.S., Boyer, L.A., Jaenisch, R., and Young, R.A. (2007). A chromatin landmark and transcription initiation at most promoters in human cells. Cell *130*, 77–88.

He, S., Tong, Q., Bishop, D.K., and Zhang, Y. (2013). Histone methyltransferase and histone methylation in inflammatory T-cell responses. Immunotherapy *5*, 989–1004.

Hosken, N.A., Shibuya, K., Heath, A.W., Murphy, K.M., and O'Garra, A. (1995). The effect of antigen dose on CD4+ T helper cell phenotype development in a T cell receptor-alpha beta-transgenic model. J. Exp. Med. *182*, 1579–1584.

Hoyne, G.F., O'Hehir, R.E., Wraith, D.C., Thomas, W.R., and Lamb, J.R. (1993). Inhibition of T cell and antibody responses to house dust mite allergen by inhalation of the dominant T cell epitope in naive and sensitized mice. J. Exp. Med. *178*, 1783–1788.

Huang, Y., Guo, L., Qiu, J., Chen, X., Hu-Li, J., Siebenlist, U., Williamson, P.R., Urban, J.F., Jr., and Paul, W.E. (2015). IL-25-responsive, lineage-negative KLRG1(hi) cells are multipotential 'inflammatory' type 2 innate lymphoid cells. Nat. Immunol. *16*, 161–169.

Im, H., Park, C., Feng, Q., Johnson, K.D., Kiekhaefer, C.M., Choi, K., Zhang, Y., and Bresnick, E.H. (2003). Dynamic regulation of histone H3 methylated at lysine 79 within a tissue-specific chromatin domain. J. Biol. Chem. *278*, 18346–18352.

Intlekofer, A.M., Banerjee, A., Takemoto, N., Gordon, S.M., Dejong, C.S., Shin, H., Hunter, C.A., Wherry, E.J., Lindsten, T., and Reiner, S.L. (2008). Anomalous type 17 response to viral infection by $CD8^+$ T cells lacking T-bet and eomesodermin. Science *321*, 408–411.

Jones, B., Su, H., Bhat, A., Lei, H., Bajko, J., Hevi, S., Baltus, G.A., Kadam, S., Zhai, H., Valdez, R., et al. (2008). The histone H3K79 methyltransferase Dot1L is essential for mammalian development and heterochromatin structure. PLoS Genet. *4*, e1000190.

Kerdiles, Y.M., Stone, E.L., Beisner, D.R., McGargill, M.A., Ch'en, I.L., Stockmann, C., Katayama, C.D., and Hedrick, S.M. (2010). Foxo transcription factors control regulatory T cell development and function. Immunity *33*, 890–904.

Kim, E.H., Gasper, D.J., Lee, S.H., Plisch, E.H., Svaren, J., and Suresh, M. (2014). Bach2 regulates homeostasis of Foxp3+ regulatory T cells and protects against fatal lung disease in mice. J. Immunol. *192*, 985–995.

Kozuka, T., Sugita, M., Shetzline, S., Gewirtz, A.M., and Nakata, Y. (2011). c-Myb and GATA-3 cooperatively regulate IL-13 expression via conserved GATA-3 response element and recruit mixed lineage leukemia (MLL) for histone modification of the IL-13 locus. J. Immunol. *187*, 5974–5982.

Kryczek, I., Lin, Y., Nagarsheth, N., Peng, D., Zhao, L., Zhao, E., Vatan, L., Szeliga, W., Dou, Y., Owens, S., et al. (2014). IL-22(+)CD4(+) T cells promote colorectal cancer stemness via STAT3 transcription factor activation and induction of the methyltransferase DOT1L. Immunity *40*, 772–784.

Kwesi-Maliepaard, E.M., Aslam, M.A., Alemdehy, M.F., van den Brand, T., McLean, C., Vlaming, H., van Welsem, T., Korthout, T., Lancini, C., Hendriks, S., et al. (2020). The histone methyltransferase DOT1L prevents antigen-independent differentiation and safeguards epigenetic identity of $CD8^+$ T cells. Proc. Natl. Acad. Sci. USA *117*, 20706–20716.

Lehnertz, B., Northrop, J.P., Antignano, F., Burrows, K., Hadidi, S., Mullaly, S.C., Rossi, F.M.V., and Zaph, C. (2010). Activating and inhibitory functions for the histone lysine methyltransferase G9a in T helper cell differentiation and function. J. Exp. Med. *207*, 915–922.

Min, J., Feng, Q., Li, Z., Zhang, Y., and Xu, R.-M. (2003). Structure of the catalytic domain of human DOT1L, a non-SET domain nucleosomal histone methyltransferase. Cell *112*, 711–723.

Mullen, A.C., High, F.A., Hutchins, A.S., Lee, H.W., Villarino, A.V., Livingston, D.M., Kung, A.L., Cereb, N., Yao, T.P., Yang, S.Y., and Reiner, S.L. (2001). Role of T-bet in commitment of TH1 cells before IL-12-dependent selection. Science *292*, 1907–1910.

Ouyang, W., Ranganath, S.H., Weindel, K., Bhattacharya, D., Murphy, T.L., Sha, W.C., and Murphy, K.M. (1998). Inhibition of Th1 development mediated by GATA-3 through an IL-4-independent mechanism. Immunity *9*, 745–755.

Peña-Rossi, C., Zuckerman, L.A., Strong, J., Kwan, J., Ferris, W., Chan, S., Tarakhovsky, A., Beyers, A.D., and Killeen, N. (1999). Negative regulation of CD4 lineage development and responses by CD5. J. Immunol. *163*, 6494–6501.

Pursani, V., Bhartiya, D., Tanavde, V., Bashir, M., and Sampath, P. (2018). Transcriptional activator DOT1L putatively regulates human embryonic stem cell differentiation into the cardiac lineage. Stem Cell Res. Ther. *9*, 97.

Ramírez, F., Ryan, D.P., Grüning, B., Bhardwaj, V., Kilpert, F., Richter, A.S., Heyne, S., Dündar, F., and Manke, T. (2016). deepTools2: a next generation web server for deep-sequencing data analysis. Nucleic Acids Res. *44* (*W1*), W160–W165.

Reinhardt, R.L., Liang, H.-E., and Locksley, R.M. (2009). Cytokine-secreting follicular T cells shape the antibody repertoire. Nat. Immunol. *10*, 385–393.

Roychoudhuri, R., Hirahara, K., Mousavi, K., Clever, D., Klebanoff, C.A., Bonelli, M., Sciumè, G., Zare, H., Vahedi, G., Dema, B., et al. (2013). BACH2 represses effector programs to stabilize T(reg)-mediated immune homeostasis. Nature *498*, 506–510.

Schapira, M., and Arrowsmith, C.H. (2016). Methyltransferase inhibitors for modulation of the epigenome and beyond. Curr. Opin. Chem. Biol. *33*, 81–87.

Scheer, S., Ackloo, S., Medina, T.S., Schapira, M., Li, F., Ward, J.A., Lewis, A.M., Northrop, J.P., Richardson, P.L., Kaniskan, H.Ü., et al. (2019). A chemical biology toolbox to study protein methyltransferases and epigenetic signaling. Nat. Commun. *10*, 19.

Schumann, J., Stanko, K., Schliesser, U., Appelt, C., and Sawitzki, B. (2015). Differences in CD44 surface expression levels and function discriminates IL-17 and IFN-γ producing helper T cells. PLoS ONE *10*, e0132479.

Sekiya, T., Kashiwagi, I., Inoue, N., Morita, R., Hori, S., Waldmann, H., Rudensky, A.Y., Ichinose, H., Metzger, D., Chambon, P., and Yoshimura, A. (2011). The nuclear orphan receptor Nr4a2 induces Foxp3 and regulates differentiation of $CD4^+$ T cells. Nat. Commun. *2*, 269.

Steger, D.J., Lefterova, M.I., Ying, L., Stonestrom, A.J., Schupp, M., Zhuo, D., Vakoc, A.L., Kim, J.-E., Chen, J., Lazar, M.A., et al. (2008). DOT1L/KMT4 recruitment and H3K79 methylation are ubiquitously coupled with gene transcription in mammalian cells. Mol. Cell. Biol. *28*, 2825–2839.

Stein, E.M., Garcia-Manero, G., Rizzieri, D.A., Tibes, R., Berdeja, J.G., Jongen-Lavrencic, M., Altman, J.K., Dohner, H., Thomson, B., Blakemore, S.J., et al. (2015). A phase 1 study of the DOT1L inhibitor, pinometostat (EPZ-5676), in adults with relapsed or refractory leukemia: safety, clinical activity, exposure and target inhibition. Blood *126*, 2547.

Stein, E.M., Garcia-Manero, G., Rizzieri, D.A., Tibes, R., Berdeja, J.G., Savona, M.R., Jongen-Lavrenic, M., Altman, J.K., Thomson, B., Blakemore, S.J., et al. (2018). The DOT1L inhibitor pinometostat reduces H3K79 methylation and has modest clinical activity in adult acute leukemia. Blood *131*, 2661–2669.

Stubbington, M.J., Mahata, B., Svensson, V., Deonarine, A., Nissen, J.K., Betz, A.G., and Teichmann, S.A. (2015). An atlas of mouse CD4(+) T cell transcriptomes. Biol. Direct *10*, 14.

Szabo, S.J., Kim, S.T., Costa, G.L., Zhang, X., Fathman, C.G., and Glimcher, L.H. (2000). A novel transcription factor, T-bet, directs Th1 lineage commitment. Cell *100*, 655–669.

Szabo, S.J., Sullivan, B.M., Stemmann, C., Satoskar, A.R., Sleckman, B.P., and Glimcher, L.H. (2002). Distinct effects of T-bet in TH1 lineage commitment and IFN-gamma production in CD4 and CD8 T cells. Science *295*, 338–342.

Tumes, D.J., Onodera, A., Suzuki, A., Shinoda, K., Endo, Y., Iwamura, C., Hosokawa, H., Koseki, H., Tokoyoda, K., Suzuki, Y., et al. (2013). The polycomb protein Ezh2 regulates differentiation and plasticity of CD4(+) T helper type 1 and type 2 cells. Immunity *39*, 819–832.

van Panhuys, N., Klauschen, F., and Germain, R.N. (2014). T-cell-receptor-dependent signal intensity dominantly controls CD4(+) T cell polarization In Vivo. Immunity *41*, 63–74.

Voehringer, D., Liang, H.-E., and Locksley, R.M. (2008). Homeostasis and effector function of lymphopenia-induced "memory-like" T cells in constitutively T cell-depleted mice. J. Immunol. *180*, 4742–4753.

Voisinne, G., Gonzalez de Peredo, A., and Roncagalli, R. (2018). CD5, an undercover regulator of TCR signaling. Front. Immunol. *9*, 2900.

Wang, Z., Zang, C., Rosenfeld, J.A., Schones, D.E., Barski, A., Cuddapah, S., Cui, K., Roh, T.-Y., Peng, W., Zhang, M.Q., and Zhao, K. (2008). Combinatorial patterns of histone acetylations and methylations in the human genome. Nat. Genet. *40*, 897–903.

Wang, X., Wang, H., Xu, B., Jiang, D., Huang, S., Yu, H., Wu, Z., and Wu, Q. (2019). Depletion of H3K79 methyltransferase Dot1L promotes cell invasion and cancer stem-like cell property in ovarian cancer. Am. J. Transl. Res. *11*, 1145–1153.

Yang, C., Huang, X.-R., Fung, E., Liu, H.-F., and Lan, H.-Y. (2017). The regulatory T-cell transcription factor Foxp3 protects against crescentic glomerulonephritis. Sci. Rep. *7*, 1481.

Zhang, W., Xia, X., Jalal, D.I., Kuncewicz, T., Xu, W., Lesage, G.D., and Kone, B.C. (2006). Aldosterone-sensitive repression of ENaCα transcription by a histone H3 lysine-79 methyltransferase. Am. J. Physiol. Cell Physiol. *290*, C936–C946.

Zhu, J., Yamane, H., and Paul, W.E. (2010). Differentiation of effector CD4 T cell populations. Annu. Rev. Immunol. *28*, 445–489.

STAR★METHODS

KEY RESOURCES TABLE

REAGENT or RESOURCE	SOURCE	IDENTIFIER
Antibodies		
CD3 purified	Thermo Fisher Scientific	Cat# 16-0031-86, RRID:AB_468849
CD3 eFluor450	Thermo Fisher Scientific	Cat# 48-0031-82, RRID:AB_10735092
CD4 APCeFluor780	Thermo Fisher Scientific	Cat# 56-0041-82, RRID:AB_493999
CD5 FITC	Thermo Fisher Scientific	Cat# 11-0051-85, RRID:AB_464909
CD8 PE	Thermo Fisher Scientific	Cat# 12-0081-83, RRID:AB_465531
CD19 FITC	Thermo Fisher Scientific	Cat# 11-0193-85, RRID:AB_657668
CD45.1 BV711	BioLegend	Cat# 110739, RRID:AB_2562605
CD45.2 APCCy7	BioLegend	Cat# 109824, RRID:AB_830789
CD44 eFluor450	Thermo Fisher Scientific	Cat# 48-0441-82, RRID:AB_1272246
CD62L APC	Thermo Fisher Scientific	Cat# 17-0621-82, RRID:AB_469410
Ki67 PE	Thermo Fisher Scientific	Cat# 12-5698-82, RRID:AB_11150954
CD69 PECy7	TONBO	Cat#60-0691-U100, RRID: N/A
GATA3 PE	Thermo Fisher Scientific	Cat# 12-9966-42, RRID:AB_1963600
IFNγ PECy7	Thermo Fisher Scientific	Cat# 25-7311-82, RRID:AB_469680
IFNγ purified	Thermo Fisher Scientific	Cat# 14-7311-81, RRID:AB_468467
CD28 purified	Thermo Fisher Scientific	Cat# 16-0281-86, RRID:AB_468923
IL-13 purified	Thermo Fisher Scientific	Cat# 14-7133-81, RRID:AB_763553
IL-13 biotin	Thermo Fisher Scientific	Cat# 13-7135-81, RRID:AB_763555
IL-4 purified	Thermo Fisher Scientific	Cat# 14-7041-81, RRID:AB_468410
IL-4 biotin	Thermo Fisher Scientific	Cat# 13-7042-81, RRID:AB_466902
IL-17 APC	Thermo Fisher Scientific	Cat# 17-7177-81, RRID:AB_763580
PD-1 APC	Thermo Fisher Scientific	Cat# 17-9985-82, RRID:AB_11149358
Nur77 PE	Thermo Fisher Scientific	Cat# 12-5965-82, RRID:AB_1257209
CXCR5 PECy7	BioLegend	Cat# 145516, RRID:AB_2562210
RORγ APC	Thermo Fisher Scientific	Cat# 17-6981-82, RRID:AB_2573254
TBET APC	Thermo Fisher Scientific	Cat# 50-5825-82, RRID:AB_10596655
Streptavidin HRP	Thermo Fisher Scientific	Cat#N100, RRID: N/A
H3K79me2	Abcam	Cat# ab3594, RRID:AB_303937
panH3	Abcam	Cat# ab1791, RRID:AB_302613
Other reagents		
CellTrace Far Red Cell Proliferation Kit	Thermo Fisher Scientific	Cat# C34572, RRID: N/A
Chemicals, Peptides, and Recombinant Proteins		
Mouse IL-1β recombinant protein carrier-free	Thermo Fisher Scientific	Cat# 34-8012-85, RRID: N/A
Mouse IL-2 recombinant protein carrier-free	Thermo Fisher Scientific	Cat# 34-8021-85, RRID: N/A
Mouse IL-4 recombinant protein carrier-free	Thermo Fisher Scientific	Cat# 34-8041-85, RRID: N/A
Mouse IL-6 recombinant protein carrier-free	Thermo Fisher Scientific	Cat# 34-8061-85, RRID: N/A
Mouse IL-12p70 recombinant protein carrier-free	Thermo Fisher Scientific	Cat# 34-8121-85, RRID: N/A
Mouse IL-23 recombinant protein carrier-free	Thermo Fisher Scientific	Cat# 34-8231-85, RRID: N/A

(*Continued on next page*)

Continued

REAGENT or RESOURCE	SOURCE	IDENTIFIER
Mouse TNF recombinant protein carrier-free	Thermo Fisher Scientific	Cat# 34-8321-85, RRID: N/A
Mouse TGF-β recombinant protein carrier-free	Thermo Fisher Scientific	Cat# 34-8342-85, RRID: N/A
Critical Commercial Assays		
Nucleospin RNA kit	Macherey-Nagel	Cat# 740955.250, RRID: N/A
Nucleospin Gel and PCR Clean-up kit	Macherey-Nagel	Cat# 740609.250, RRID: N/A
Deposited Data		
RNA-seq	this study	GSE123966
ChIP-seq	this study	GSE138821
Experimental Models: Organisms/Strains		
Mouse: Ly5.1: B6.SJL-*Ptprc*^{a} *Pepc*^{b}/BoyJ	originally obtained from The Jackson Laboratory and then maintained by breeding in our facility	PMID: 3864163,
Mouse: DOT1L$^{\Delta T}$: Dot1l$^{tm1a(KOMP)Wtsi}$	Rederived from ES cells in house and crossed to CD4Cre mice.	RRID: MMRRC_054749-UCD
Mouse: TBET$^{\Delta T}$: B6.129-*TBX21*^{tm2Srnr}/J	TBET$^{FL/FL}$ mice were kindly provided by Dr Joanna Groom and crossed to CD4Cre mice in house.	JAX stock #022741
Mouse: CRY: Tg(Il4-AmCyan,Il13-DsRed*) 1Wep x C.129S4(B6)-*Ifng*$^{tm3.1Lky}$/J	4C13R mice were kindly provided by Dr Simon Phipps; IFN-γ reporter mice were kindly provided by Dr Di Yu. 4C13R and GREAT mice were crossed with CD4Cre mice in house.	(Huang et al., 2015), (Reinhardt et al., 2009)
Oligonucleotides		
See Table S2.		
Software and Algorithms		
GraphPad PRISM 8.0		https://www.graphpad.com/scientificsoftware/prism/
GALAXY		https://www.usegalaxy.org
FlowJo v10		https://www.flowjo.com/solutions/flowjo

RESOURCE AVAILABILITY

Lead contact

Further information and requests for resources and reagents should be directed to and will be fulfilled by the Lead Contact, Colby Zaph (colby.zaph@monash.edu)

Materials availability

This study did not generate any new unique reagents.

Data and code availability

RNA-Seq and ChIP-Seq datasets generated in this study are available at the National Center for Biotechnology Information (GEO: GSE123966, GSE138821, respectively).

EXPERIMENTAL MODEL AND SUBJECT DETAILS

To create DOT1L$^{FL/FL}$ mice, we derived mice from DOT1L targeted ES cells (Dot1ltm1a(KOMP)Wtsi) and crossed them with FLP mice (Monash University). Subsequently, DOT1L$^{FL/FL}$ mice were crossed with *Cd4*-Cre^{+} (C57BL/6 background) to generate DOT1L$^{\Delta T}$ mice. DOT1L$^{\Delta T}$ mice were crossed with IFN-γ-YFP reporter mice (Reinhardt et al., 2009) to create DOT1L$^{\Delta T}$IFN-γYFP mice. DOT1L$^{\Delta T}$CRY mice were generated by crossing DOT1L$^{\Delta T}$IFN-γYFP with 4C13R (Huang et al., 2015) mice. DOT1L/TBET$^{\Delta T}$ mice were created by crossing DOT1L$^{\Delta T}$ and TBET$^{\Delta T}$ (Intlekofer et al., 2008). For transfer experiments, naive (CD44^{-} CD62L^{high}) cells

from either Ly5.1/2 or DOT1L$^{\Delta T}$ mice were sorted and injected intraperitoneally into DOT1L$^{FL/FL}$ or DOT1L$^{\Delta T}$, or Ly5.1/2, respectively, before analysis 5-7 days later. Female and male animals were used throughout this study, were maintained in a specific pathogen-free environment and used at 6-10 weeks of age. Animals were maintained in a specific pathogen-free environment and used at 6-10 weeks of age. Experiments and the animals' care were in accordance with the animal ethics committee of Monash University.

METHOD DETAILS

Mixed bone marrow chimeras

Mixed bone marrow (mBM) chimera mice (CD45.1 recipient) were generated using 50:50 BM from WT congenic (CD45.1/.2) and DOT1L$^{\Delta T}$ (CD45.2) mice and analyzed 12-16 weeks after reconstitution.

House dust mite (HDM) model of allergic asthma

For the first 3 days of airway sensitization, mice were anesthetized under aerosolized isoflurane and intranasally instilled daily with 100 μg of house dust mite (HDM) antigen (Greer, Lenoir, NC) in 40 μl PBS. On days 13 to 17 post sensitization, mice were intranasally challenged daily with 25 μg of HDM antigen in 40 μl PBS before analysis on day 18. Bronchoalveolar lavage (BAL) was performed from the right lobes of the lung with three flushes of 800 μl PBS after clamping off the left lobe of the lung (used for histology). BAL fluid and tissues were processed as previously described (Chenery et al., 2015).

Trichuris muris infection

Propagation of *Trichuris muris* eggs and infections were performed as previously described (Antignano et al., 2011). Mice were infected with 200 embryonated *T. muris* eggs by oral gavage to induce an intestinal infection over a period of 21 days. Sacrificed mice were assessed for worm burdens by manually counting worms in the ceca using a dissecting microscope. Mesenteric lymph node cells were restimulated in the presence of αCD3/αCD28 (1 μg/ml each) for 3 days and analyzed after restimulation with cell stimulation cocktail containing protein transport inhibitor (ThermoFisher).

T cell assays

CD4$^+$ T cells were isolated from spleen and peripheral lymph nodes from indicated mice by negative selection using the EasySep Mouse CD4$^+$ T Cell Isolation Kit (StemCell Technologies Inc). 1.75 × 10^5 cells were cultured for 4 days in RPMI-1640 supplemented with 10% heat-inactivated FCS, 2 mM L-glutamine, 100 U/ml penicillin, 100 μg/ml streptomycin, 25 mM HEPES, and 5 × 10^{-5} M 2-mercaptoethanol with 1 μg/ml each of plate-bound αCD3 (clone 145-2C11) and αCD28 (clone 37.51). Cells were cultured under neutral (Th0; IL-2, 10 ng/ml), Th1 (IL-2 and IL-12, 10 ng/ml each; αIL-4 10 μg/ml), Th2 (IL-2 and IL-4, 10 ng/ml and 40 ng/ml, respectively; αIFN-γ 10 μg/ml), or Th17 (IL-1β, IL-23, TNF at 10ng/ml; IL-6 at 20 ng/ml; TGF-β at 1 ng/ml; αIL-4 and αIFN-γ at 10 μg/ml each) polarizing conditions.

Western blot

T cells (CD4$^+$ or CD8$^+$) and B cells (CD19$^+$) were sorted from the spleens of DOT1L$^{\Delta T}$ or CD4-Cre mice and pellets were frozen at −80°C. Histones were extracted from frozen cell pellets by incubating in 0.2 N HCl overnight at 4°C. Supernatants were run on 12% SDS-PAGE gels. H3K79me2 was detected using clone ab3594 (Abcam). A pan H3 antibody (ab1791, Abcam) was used as a loading control.

ELISA

T. muris-specific IgG1 was analyzed as previously described. In short, ELISA plates were coated with o/n supernatant of adult worms, blocked with 10% NCS and serum was added in serial dilutions (1/20-1/2560). Secondary antibody (IgG1-HRP) was added at 1/1000 and incubated with 50 μl of TMB substrate until adequately developed. TMB substrate reaction was stopped by adding 50 μl of 1 N HCl and the plate was read at 450 nm. IL-4 ELISA was performed with capture antibody (clone 11B11) and biotinylated detection antibody (clone BVD6-24G2). Biotin-HRP was added 1/1000 and incubated with 50 μl of TMB substrate until adequately developed. TMB substrate reaction was stopped by adding 50 μl of 1 N HCl and the plate was read at 450 nm.

RNA-sequencing

RNA was isolated from viable bona fide Th1 (YFP$^+$) or viable Th2 polarized cells of control (CD4Cre$^+$) and DOT1L$^{\Delta T}$ mice after 4 days of culturing under Th1 and Th2 polarizing conditions, respectively, using the NucleoSpin RNA Kit from Macherey-Nagel according to the manufacturer's instructions and sequenced on a MiSeq paired-end run (75 × 75, v3; Illumina). Samples were aligned to the mm10 transcript reference using TopHat2, and differential expression was assessed using Cufflinks (Illumina). Visualization of the data was performed using DEGUST (https://github.com/drpowell/degust) and represent the average expression from two biological replicates. Raw data is available in Table S1.

Expression analysis

Expression analysis (qPCR) from the proximal colon of *T. muris*-infected mice was performed using primer pairs according to Table S2. Samples were standardized using *Actb*.

Chromatin Immunoprecipitation (ChIP)

1-1.5 × 10^6 sorted naive T cells ($CD4^+$ $CD44^-$ $CD62L^{high}$), bona fide Th1 (YFP^+) and bona fide Th2 ($AmCyan^+$/$dsRed^+$) cells from control (CRY mice) or $DOT1L^{\Delta T}$-CRY mice were fixed for 8 min at room temperature with 0.6% formaldehyde in 10 mL complete RPMI-1640 media on an overhead rotator. Fixing was stopped by adding 1 mL of 1.25 M glycine and incubating for 5 min on an overhead rotator at room temperature. Cells were pelleted at 600 x g for 5 min at 4°C and washed twice with 10 mL ice cold PBS. Pellets were resuspended in 250 μl ChIP lysis buffer and stored at −80°C. Cells were sonicated in 3 sets of 10 × 30 s ON, 30 s OFF at 4°C using a Bioruptor (Diagenode) with intermittent quick vortex and centrifugation using polystyrene tubes. 200 μl of the supernatant was collected after centrifugation at 15,000 x g for 10 min at 4°C and diluted in 800 μl ChIP dilution buffer containing 1:20 protease inhibitor. 40 μl of washed protein A and protein G magnetic beads (BioRad) and 2 μg of αH3K79me2 (ab3594) were added and incubated o/n at 4°C on an overhead rotator. 20 μl of the supernatant (input) were diluted in 180 μl ChIP dilution buffer containing 0.3 M NaCl and incubated at 65°C o/n for decrosslinking before using the PCR purification kit (Macherey-Nagel) for isolation of DNA. Next day, IP samples were washed consecutively twice with 1 mL of each ChIP low salt, ChIP high salt, ChIP LiCl and TE buffer using a magnet. Chromatin was eluted after the last wash by incubating twice with 150 μl ChIP elution buffer on an overhead rotator at room temperature. Both elutions were pooled and incubated at 65°C o/n in the presence of 0.3 M NaCl. Next day, IP samples were purified using the PCR purification kit (Macherey-Nagel) and DNA was stored at −80°C until QC and library preparation, or until ChIP-qPCR was performed.

ChIP-sequencing

ChIP samples were processed using the MGITech MGIEasy DNA FS Library preparation kit V1 (according to the manufacturer's instructions: document revision A0) and sequenced using one lane of the MGISEQ-2000RS using an MGISEQ-2000RS High-Throughput Sequencing Set (PE100), yielding paired-end 100 base reads (according to the manufacturer's instructions: document revision A1).

ChIP-qPCR

ChIP-qPCR for the *Bach2* and *Ifng* locus was performed using primer pairs according to Table S2. Input samples served as standard.

QUANTIFICATION AND STATISTICAL ANALYSIS

Statistical significance was determined by 2-tailed Student's t test or one-way-ANOVA using GraphPad Prism 8 software (GraphPad Software, La Jolla, CA, USA). Results were considered statistically significant with $p \leq 0.05$. *$p \leq 0.05$, **$p \leq 0.01$, ***$p \leq 0.001$ and can be found in the figure legends.